Isospin Mixing In Magnesium-24

by
Charles David Hoyle

A dissertation submitted in partial fulfillment
of the requirements for the degree of

Doctor of Philosophy

University of Washington
1981

DISCLAIMER

UNIVERSITY OF WASHINGTON

Date: November 24, 1981

We have carefully read the dissertation entitled
Isospin Mixing in Magnesium-24

submitted by
Charles David Hoyle
in partial fulfillment of
the requirements of the degree of Doctor of Philosophy
and recommend its acceptance. In support of this recommendation we present the following joint statement of evaluation to be filed with the dissertation.

This dissertation is a well written report of a carefully conceived and executed experiment. The result of this experiment has been the measurement of an unusually large charge-dependent effect in nuclear β decay, strongly suggesting the presence of a component of the nuclear force which breaks isospin symmetry. As such, the work reported in this dissertation represents a significant advancement in the field of Nuclear Physics.

DOE/ER/01388--513

DE82 011084

MGW

DISSERTATION READING COMMITTEE:

University of Washington

Abstract

Isospin Mixing in Magnesium-24

By Charles David Hoyle

Chairperson of the Supervisory Committee: Professor Eric G. Adelberger
Department of Physics

The β-γ circular polarization correlation asymmetry was measured for the pure Gamow-Teller decay of ^{28}Al, for the pure Fermi decay of ^{14}O and for the mixed decay of the ^{24}Al 4^+ ground state to the 8.437 MeV, 4^+ state in ^{24}Mg. The expected results were obtained for the pure Gamow-Teller and Fermi decays. From the results of the ^{24}Al decay the isospin mixing of the 8.437 MeV, 4^+ state and the 9.515 MeV, 4^+ analog state in ^{24}Mg was determined. The charge dependent matrix element mixing these two states was determined to be -95 ± 36 keV. This is the largest charge dependent matrix element observed in β decay to date. This large value has not been completely explained and suggests the existence of a $\Delta T=1$ nuclear force.

Isospin Mixing In Magnesium-24

by

Charles David Hoyle

A dissertation submitted in partial fulfillment
of the requirements for the degree of

Doctor of Philosophy

University of Washington

1981

Approved by Eric H. Rehm Hinrichsen
(Chairperson of Supervisory Committee)

Program Authorized
to Offer Degree Department of Physics

Date November 25, 1981

Doctoral Dissertation

In presenting this dissertation in partial fulfillment of the requirements for the Doctoral degree at the University of Washington, I agree that the Library shall make its copies freely available for inspection. I further agree that extensive copying of this dissertation is allowable only for scholarly purposes, consistent with "fair use" as prescribed in the U.S. Copyright Law. Requests for copying or reproduction of this dissertation may be referred to University Microfilms, 300 North Zeeb Road, Ann Arbor, Michigan 48106, to whom the author has granted "the right to reproduce and sell (a) copies of the manuscript in microform and/or (b) printed copies of the manuscript made from microform."

Signature Charles David Hoyle

Date May 25, 1981

ACKNOWLEDGMENTS

I wish to express a sincere appreciation to all who contributed to this work. A special thanks goes to Louie Geissel for his many hours of help in the student shop, to Rick Von Lintig, Eric Swanson and Kurt Snover for their help in setting up the experiment and taking the data, to John Blair for his theoretical help and to Tom Trainor for his careful reading of the manuscript. My greatest thanks goes to Eric Adelberger. Eric's technical and theoretical guidance along with his willingness to spend many late nights in the laboratory were essential to the completion of this work. Finally I want to thank my wife Paige for her constant encouragement which has been a great help over the last few years.

TABLE OF CONTENTS

LIST OF FIGURES

LIST OF TABLES

CHAPTER I

MOTIVATION AND THEORY

A. Introduction

After the discovery of the neutron, Heisenberg (He 32) immediately characterized the neutron and the proton as fundamental constituents of the nucleus so similar that the two particles could be thought of as different states of the same particle, the nucleon. The mathematical description of a two-state system was already available in the Pauli spin matrices. Heisenberg applied the same mathematical formalism to the description of the neutron and proton. In this way, the concept of isospin was introduced as a convenient labelling device for neutrons and protons.

Not long after the introduction of isospin in nuclear physics it became apparent for a number of reasons (An 69,Fo 66,Wi 69 and references therein) that the nuclear forces between two neutrons, two protons and a neutron and proton were approximately equal when the nucleons were in the same relative space-spin state. This early approximate charge independence of the nuclear force suggested the existence of a fundamental symmetry of the strong interaction in isospin (charge) space. To fully understand the strong interaction the degree to which this symmetry is broken must be determined.

In nuclei if the isospin symmetry is unbroken each nuclear state should be characterized by isospin quantum numbers. However, since protons are charged particles, the total Hamiltonian of a system of

neutrons and protons will break the isospin symmetry due to the relatively weak Coulomb interaction among the protons. To understand the strong interaction in nuclei one must determine the extent of isospin breaking and how much of this breaking is due to the Coulomb interaction.

The focus of this work is the measurement of isospin mixing using β-γ circular polarization correlation techniques. The β-γ circular polarization correlation technique provides a very straightforward method of measuring isospin mixing in nuclei. To put this in perspective a brief description of some of the more significant cases of isospin mixing measured by other techniques will be discussed before developing the β-γ circular polarization correlation method.

B. Isospin Formalism

Treating the neutron and proton as different states of the same particle, the nucleon, and assuming that the strong interaction is charge independent implies the existence of conserved isospin quantum numbers. The mathematical description of the two states of the nucleon in isospin space (charge space) is equivalent to the Pauli formalism for a spin-1/2 particle. The only changes necessary in the formalism are the relabelling of the states and operators. The proton is assigned a total isospin quantum number $t=1/2$ and a z-projection $t_z=1/2$. The neutron has $t=1/2$ and $t_z=-1/2$, and isospin kets are represented by $|t,t_z\rangle$. The isospin operator $\vec{t}=1/2\,\vec{\tau}$ is defined in complete analogy with the Pauli spin operators, with $\vec{\tau}$ having the same

representation as the Pauli $\vec{\sigma}$. Hence, the isospin operators satisfy all the commutation relations and vector addition rules of angular momentum.

The nucleon charge operator is given by $q = e(t_z + 1/2)$ which acting on nucleon states gives $q|\text{proton}\rangle = q|1/2,1/2\rangle = e|\text{proton}\rangle$ and $q|\text{neutron}\rangle = q|1/2,-1/2\rangle = 0$. The total isospin operator for a nucleus with A nucleons is given by $\vec{T} = \sum_i \vec{t}_i$, and the total charge operator is given by $\sum_i q_i = \sum_i e(t_{zi} + 1/2) = e(T_z + A/2)$ where the sum over the index i is the sum over operators for all individual nucleons. Since T_z has this simple relation to the total charge of the nucleus the assignment of T_z quantum numbers to any nuclear state is simple.

The assignment of a total isospin quantum number is not so simple. For a nucleus of A nucleons and complete charge independence, T can take on any value between |N-Z| and A/2 where N = the number of neutrons. For most nuclei the ground state has $T=T_z$, but there are exceptions to this rule (e.g. ^{34}Cl and ^{42}Sc both have T=1 ground states). Many techniques have been used to determine the value of T for many nuclear states (Wi 69, En 78). With a small isospin symmetry breaking perturbation the physical states of nuclei should no longer be described by a single T quantum number. The new physical states will be the unperturbed states with small admixtures of states with different values of T. The measurement of the isospin mixing in the physical nuclear states is a measurement of isospin symmetry breaking.

C. Direct-Reaction Studies of Isospin Mixing

One of the earliest approaches to the determination of isospin mixing involved the direct reaction $^{10}B(d,\alpha)^{8}Be^{*}$. The mixing of the two 2^{+} states in ^{8}Be at 16.6 and 16.9 MeV was studied using many reactions. A review of all the reactions used to study this mixing is given in reference Ma 66. The $^{10}B(d,\alpha)^{8}Be^{*}$ reaction was used by Erskine and Brown to study the isospin mixing of the two 2^{+} states and is representative of the problems encountered and success possible with particle reaction studies (Er 61,Er 66 and Br 66).

From binding energy considerations, Erskine and Brown expected the lowest T=1 state in ^{8}Be to be either the 16.6 or the 16.9 Mev state. Dietrich and Cranberg (Di 60) had measured the absolute cross section and angular distribution of the $^{7}Li(d,n)^{8}Be$ and $^{7}Li(d,p)^{8}Li$ analog reactions. The results of these measurements indicated that the 16.6 MeV state was the T=1 analog of the ^{8}Li ground state. The spacing of these levels was so close that a small charge-dependent matrix element between these two states could produce much isospin mixing.

Since the deuteron, alpha particle, and ^{10}B ground state all have T=0 the formation of $^{8}Be^{*}$ states with T=1 should be greatly inhibited for a charge-independent nuclear force. Therefore, the lowest T=1 state should produce a much smaller yield of α particles. Erskine and Brown measured the cross section for the $^{10}B(d,\alpha)^{8}Be^{*}$(16.6 Mev) and $^{10}B(d,\alpha)^{8}Be^{*}$(16.9 Mev) reactions and found the cross sections to be nearly equal, implying that the 16.6 and 16.9 MeV states were nearly

equal mixtures of T=0 and T=1 states. The cross section ratio was measured at several energies. The constancy of the cross section ratio suggested that the two states were produced almost equally due to the isospin mixing of the states and not some isospin dependence of the reaction mechanism.

To obtain a quantitative measure of the isospin mixing it was assumed that the wave functions for the two states could be written as

$$|16.6\text{Mev}\rangle = \alpha|T=0,T_z=0\rangle + \beta|T=1,T=0\rangle$$

$$|16.9\ \text{Mev}\rangle = \beta|T=0,T_z=0\rangle - \alpha|T=1,T=0\rangle$$

where $\alpha^2+\beta^2=1$ and the isospin states are the pure states that would exist in the absence of all charge dependent forces. An approximate theory of line shapes (Br 66) was then used to fit the observed α particle line shapes and determine the quantities α and β. Six parameters were varied in the model until the best fit to the data was obtained. This procedure yielded

$$\alpha = 0.763$$

and

$$\beta = 0.647.$$

Brown used these values and a procedure due to Barker (Ba 66) to calculate the charge-dependent matrix element necessary to produce the observed mixing. This procedure yielded a matrix element of -143 keV. Using only the Coulomb force and the measured mixing of the T=1 and T=0 states, Barker (Ba 66) calculated the same matrix element, using an intermediate coupling shell model, to be -67 keV. From this Barker concluded that addition configuration mixing or a more complicated force was needed to explain the observed mixing.

Direct reaction studies were also used in the study of the isospin mixing between the 1^+, T=0 state at 12.7 MeV and the 1^+, T=1 state at 15.1 MeV in ^{12}C (Br 72, Li 77). Again the physical states were expanded in terms of isospin eigenstates to give

$$|15.1\ \text{Mev}\rangle = \alpha|T=1,T_z=0\rangle + \beta|T=0,T_z=0\rangle$$

$$|12.7\ \text{Mev}\rangle = -\beta|T=1,T_z=0\rangle + \alpha|T=0,T_z=0\rangle$$

with $\beta = \langle T=1,T_z=0|H_{CD}|T=0,T_z=0\rangle/(E_1-E_0)$

$\alpha = (1-\beta^2)^{1/2}$

H_{CD} = charge dependent part of the Hamiltonian

$E_{1(0)}$ = energy of the T=1(0) state.

In this case the energy separation of the two states is much larger than the separation of the levels in ^8Be. Hence, the resulting mixing will be smaller and considerable care must be taken in extracting the charge-dependent matrix element.

The isospin mixing of the two states was determined using the analog reactions $^{13}C(d,t)^{12}C^*(15.1\ \text{Mev})$ and $^{13}C(d,^3He)^{12}B(\text{ground state})$. Assuming charge independence, the initial state for both reactions is given by

$$|^{13}C,T=1/2,T_z=-1/2\rangle|d,T=0,T_z=0\rangle = |T=1/2,T_z=-1/2\rangle.$$

The final state for the first reaction is given by

$$|^{12}C,T=1,T_z=0\rangle|t,T=1/2,T_z=-1/2\rangle = (3/2,-1/2|1,0,1/2,-1/2)|3/2,-1/2\rangle$$

$$+ (1/2,-1/2,|1,0,1/2,-1/2)|1/2,-1/2\rangle$$

and the final state for the second reaction is given by

$$|^{12}B,T=1,T_z=-1\rangle|^3He,T=1/2,T_z=1/2\rangle = (3/2,-1/2|1,-1,1/2,1/2)|3/2,-1/2\rangle + (1/2,-1/2|1,-1,1/2,1/2)|1/2,-1/2\rangle.$$

where the quantities in parentheses are the usual vector coupling coefficients. The ratio of cross sections for the two reactions is given by the ratio of the squares of the overlaps of the initial and final states, implying

$$\frac{d\sigma(d,t)/d\Omega}{d\sigma(d,^3He)/d\Omega} = \frac{|(1/2,-1/2|1,0,1/2,-1/2)|^2}{|(3/2,-1/2|1,-1,1/2,1/2)|^2}$$

$$= (1/3)/(2/3) = 1/2.$$

This ratio will be modified by isospin mixing of the 12.7 MeV and 15.1 MeV states as well as other effects. Two of the more important effects are the difference in Coulomb interaction of the outgoing t and ^3He and the difference in pickup amplitudes for the neutron and proton. Since the (d,t) reaction can form both T=1 and T=0 states in ^{12}C isospin mixing can lead to interference effects in the pickup amplitudes in this reaction.

To extract $\langle H_{CD}\rangle$, Braithwaite et al. used the DWBA approximation to calculate the expected ratio of cross sections. The ratio of the $p_{1/2}$ to the $p_{3/2}$ pickup amplitudes was calculated using the fractional parentage coefficients of Cohen and Kurath (Co 67). With this procedure a very model-dependent charge dependent matrix element of 250 ± 50 keV was deduced. Lind et al. used the DWBA approximation

and more sophisticated wave functions (Li 77) to find a charge dependent matrix element of 179 ± 75 keV.

In summary, while direct particle reactions provide a method of measuring isospin mixing, the interpretation of the results of particle reactions is complicated. To determine isospin mixing from the particle reactions $^{13}C(d,t)^{12}C$ and $^{13}C(d,^{3}He)^{12}C$ one needs a good theory of reaction mechanisms. Since such a theory is usually taken to be the DWBA, one must assume that there is no compound nucleus formed, no isospin breaking in the reaction mechanism and a nuclear model must be employed to provide wave functions that are used to calculate observables. The isospin mixing of the model wave functions can then be varied until the model predicts the correct result for the experiment and the isospin mixing is determined. As will be shown below, the β-γ circular polarization correlation technique does not require any knowledge of nuclear reaction mechanisms and provides a completely model independent way to determine the isospin mixing.

D. M1 Decay Studies of Isospin Mixing

M1 γ decays provide another method for measuring isospin mixing. The M1 operator is given by (De 74)

$$\vec{\mu} = \mu_o \sum_i \vec{l}_i(1+\tau_{zi}) + \vec{s}_i((g_p+g_n) + \tau_{zi}(g_p-g_n))/2$$

where μ_o = the nuclear magneton

g_p = gyromagnetic ratio of the proton

g_n = gyromagnetic ratio of the neutron

$(g_p+g_n)/2 = 0.88$

$$(g_p - g_n)/2 = 4.71$$

Dividing up the M1 operator into its isoscalar and isovector parts gives

$$\vec{\mu} = \vec{\mu}_s + \vec{\mu}_v$$

with $\vec{\mu}_s = \mu_o/2 \sum_i (\vec{j}_i + (g_p+g_n-1)\vec{s}_i)$

$$\vec{\mu}_v = \mu_o/2 \sum_i \tau_{zi}(\vec{l}_i+(g_p-g_n)\vec{s}_i)$$

with the isoscalar part being relatively small due to the small value of g_p+g_n. The selection rules for the M1 operator are that the M1 matrix element vanishes unless $\Delta J = \pm 1,0$ (no $0 \rightarrow 0$) and $\Delta T = \pm 1,0$. In addition to these selection rules, M1 transitions with $\Delta T=0$ in $T_z=0$ nuclei are smaller by about a factor of 100 compared to normal M1 transitions (Mo 58) due to the almost complete cancellation of the neutron and proton magnetic moments in the factor $g_p + g_n - 1$ (= .38).

The isospin mixing of the 16.6 and 16.9 MeV states in ^{8}Be was studied by two groups (Pa 68, Sw 68) using M1 transitions to these states. The two 1^+ states at 18.2 and 17.6 MeV in ^{8}Be were populated using the ^{7}Li(p,γ)^{8}Be* reaction. The γ rays from these states were then detected in coincidence with the α particles from the breakup of the ^{8}Be excited states at 16.6 and 16.9 MeV. The rates for the M1 18.2 MeV $\rightarrow$ 16.6 MeV, 18.2 MeV $\rightarrow$ 16.9 MeV, 17.6 MeV $\rightarrow$ 16.6 MeV and 17.6 MeV $\rightarrow$ 16.9 MeV transitions were all measured by Paul et al. (Pa 68). The wave functions for the four states involved were assumed to be of the form

$$|2^+, 16.6 \text{ MeV}\rangle = \alpha|2^+,0,0\rangle + \beta|2^+,1,0\rangle$$

$$|2^+, 16.9 \text{ MeV}\rangle = \beta|2^+,0,0\rangle - \alpha|2^+,1,0\rangle$$

$$|1^+, 17.6 \text{ MeV}\rangle = \gamma|1^+,0,0\rangle + \delta|1^+,1,0\rangle$$

$$|1^+, 18.2 \text{ MeV}\rangle = \delta|1^+,0,0\rangle - \gamma|1^+,1,0\rangle$$

with $\alpha^2 + \beta^2 = 1$ and $\gamma^2 + \delta^2 = 1$. In this case the transition rates are very sensitive to the amount of isospin mixing. If the physical states were pure isospin states, the transitions with $\Delta T = 0$ should be greatly inhibited as explained above. Any mixing of the states then allows both $\Delta T = 1$ and $\Delta T = 0$ amplitudes, where only a $\Delta T = 0$ is allowed in the pure states. Since the $\Delta T = 1$ amplitude is in general much larger, a small mixing is expected to produce a sizeable change in the transition rate.

The shell model was used to calculate the M1 rates. It was assumed that there was an accidental degeneracy between the 16.6 and 16.9 MeV states that was removed by the Coulomb interaction. The isospin mixing amplitudes were then adjusted until the predicted yields agreed with the measured yields. From this analysis, Paul et al. determined that

$$\alpha = 0.773$$

$$\beta = 0.636$$

$$\gamma^2 = 0.05$$

$$\delta^2 = 0.95$$

which agree reasonably well with the results of Erskine and Brown. The wave functions associated with these mixing amplitudes were also used to predict the strengths of other transitions from the 18.2 and 17.6 MeV states. The agreement with the experimental results was not entirely adequate and further modifications to the model were made to correct for the differences (Pa 68). From this analysis Paul et al. concluded that the large isospin mixing in ^{8}Be was due primarily to

the Coulomb interaction and not due to the breakdown of isospin symmetry.

The mixing of the lowest 1^+ states in ^{12}C at 12.7 and 15.1 MeV was also studied using M1 transitions (Ad 77). The 1^+ 12.7 MeV state is predominantly T=0 and the 1^+ 15.1 MeV state is predominantly T=1. If the 12.7 MeV state was pure T = 0, the M1 transitions to lower states would be purely isoscalar decays. With the isovector part of the M1 operator being much larger than the isoscalar part, a small mixing of the T = 1 state into the T = 0 state can produce a considerable change in the M1 matrix element and transition rate.

Adelberger et al. produced excited states of ^{12}C in the $^{10}B(^3He,p)^{12}C$ and $^{11}B(p,\gamma)$ reactions and measured the relative radiative widths of the 12.7 MeV state. The results of these measurements combined with the ground state M1 transition width of the 12.7 MeV state measured by Cecil et al. (Ce 74) using the $^{12}C(e,e')$ reaction were then analyzed assuming that

$$|15.1\ \text{MeV}\rangle = \alpha|1,0\rangle + \beta|0,0\rangle$$

$$|12.7\ \text{MeV}\rangle = -\beta|1,0\rangle + \alpha|0,0\rangle$$

where $\beta/\alpha = \langle 1,0|H_{CD}|0,0\rangle/2.4\ \text{MeV}$

$$\alpha^2 + \beta^2 = 1.$$

To determine β and α, the isoscalar M1 matrix element must be calculated using a nuclear model. Therefore, the accuracy of determining β and α is limited by how accurately the isoscalar M1 amplitude for the decay of the 12.7 MeV state can be calculated. The M1 isoscalar amplitude cannot be determined from experiment since it always adds coherently with the sought-after isovector amplitude.

The model wave functions were tested on other radiative transitions in ^{12}C to see how well they did in predicting the observed rates. The wave functions that gave the best results for other transitions were then used to calculate the M1 isoscalar amplitude. Using this method Adelberger et al. deduced a charge dependent matrix element of 110 ± 30 keV which is larger than the predicted (Li 77) 50 keV due to the Coulomb force, disagrees with the 250 ± 50 keV of Braithwaite et al., agrees with the 179 ± 75 keV of Lind et al. and almost equals the 143 keV value for ^{8}Be.

It should be noted that in the case of ^{8}Be both particle reactions and γ-ray studies produced consistent results for the isospin mixing in the 16.6 and 16.9 MeV states. For the case of ^{12}C the γ-ray studies and particle reaction studies produced quite different results for the mixing of the 12.7 and 15.1 MeV states. From this one concludes that some of the assumptions made for particle reactions are subject to errors that can be large compared to the isospin mixing effects when the isospin impurities are on the order of 1% or less in intensity. This is due to the fact that the understanding of nuclear reactions has not progressed far enough to adequately predict results to the accuracy necessary for the study of isospin mixing.

The study of isospin mixing using M1 decays provides a method that does not require a reaction mechanism model but does require a nuclear model to provide wave functions for the calculation of M1 matrix elements and transition rates. These wave functions can be tested on other γ-ray transitions and particle reactions to determine

how well they correspond to physical states. In this way reasonable wave functions are selected, but the dependence on a nuclear model is still required.

E. Beta Decay Formalism

Isospin forbidden Fermi beta decays provide a method of measuring isospin mixing that does not depend on nuclear reaction mechanisms or nuclear models. For all the beta decays considered in this work, $v/c \ll 1$ for the nucleons and the wavelength of the leptons is much greater than the nuclear radius, implying that the "allowed" approximation (Wu 66, Sc 66) is quite good for all decays. In the allowed approximation there are two amplitudes for beta decay. The amplitude due to the vector current is the Fermi matrix element and the amplitude due to the axial vector current is the Gamow-Teller matrix element. Using perturbation theory and summing over all angular momentum orientations gives the well known expression for the comparative half life of an allowed beta decay (Ra 75),

$$ft = \frac{K}{G_V^2 M_F^2 + G_A^2 M_{GT}^2} \qquad \text{I.E-1}$$

where t = the experimental half life

G_V = weak interaction vector coupling constant

G_A = weak interaction axial vector coupling constant

$M_F = \langle f || \sum_n t_{\pm n} || i \rangle$

$= \langle f || T_{\pm} || i \rangle$

= Fermi matrix element

$M_{GT} = \langle f || \sum_n t_{\pm n} \vec{\sigma}_n || i \rangle$

= Gamow-Teller matrix element

$C_A/C_V = -1.25 \pm 0.01$

and the subscript n indicates summation over individual nucleon operators and the || indicates that the matrix elements are reduced in spin-orbit space only. The integrated Fermi factor f is given by

$$f = \int_1^{W_o} pW(W_o - W)^2 F(Z,W)\, dW$$

where p = beta momentum

W = beta energy in units of $m_o c^2$

F(Z,W) = Fermi function defined in terms of electron wave functions

Z = atomic number of daughter nucleus.

$K = (2\pi^3(\ln 2)\hbar^7)/(m_o^5 c^4)$

The selection rules (Sc 66, Wu 66) for determining which matrix elements contribute for a particular beta decay are

$M_F \neq 0$ if $\Delta J = 0$

$\Delta T = 0$ (i.e. both states must lie in same isospin multiplet)

$\pi_i \pi_f = +1$

$M_{GT} \neq 0$ if $\Delta J = 0, \pm 1$ (no $0 \rightarrow 0$)

$\Delta T = 0, \pm 1$ (no $0 \rightarrow 0$)

$\pi_i \pi_f = +1$

where $\pi_{i(f)}$ is the parity of the initial(final) state.

If there were no charge dependent forces and physical nuclear

states were simultaneously eigenstates of $\vec{T}$ and the nuclear Hamiltonian, these selection rules would require the Fermi matrix element between two nuclear states of different T to vanish. Since there is a small Coulomb term and probably a small charge dependent strong interaction term in the Hamiltonian the physical nuclear states are not eigenstates of $\vec{T}$. Using perturbation theory with the charge dependent part of H as the perturbation the physical states can be expanded in terms of unperturbed eigenstates of $\vec{T}$ and H. With this type of expansion the physical state is expressed as an eigenstate of T and H with small admixtures of eigenstates with different eigenvalues of T and H. With the existence of mixed states the selection rules given above are not strictly obeyed. A state that has been identified as a T=0 state may have a small T=1 admixture. Due to this small T=1 admixture the T=0 state may have a small Fermi matrix element with a T=1 state. This type of Fermi matrix element between a predominantly T=0 state and a predominantly T=1 state is called an isospin forbidden Fermi matrix element. The measurement of an isospin forbidden Fermi matrix element for a transition between mixed states provides a particularly clean and simple determination of the isospin mixing amplitude (in the usual case the mixing amplitude between the daughter state and the isospin analog of the parent state is measured).

A summary of experimentally determined isospin mixing matrix elements inferred from isospin forbidden Fermi decays has been given by Raman et al. (Ra 75). The measured matrix elements range from $0.02\ ^{+0.05}_{-0.02}$ to 56 ± 12 keV with most less than 20 keV.

Unfortunately most of the cases studied have not been treated theoretically, and hence it is difficult to draw quantitative conclusions about the possible importance of charge dependent nuclear forces from the measured effects in these nuclei. There are very few examples of measurements in light nuclei where the structure is simple enough that one can test whether or not Coulomb forces alone can account for the observed mixing. One example occurs in ^{28}Al.

The isospin mixing of the 0^+, T=1 state at 0.972 MeV with the 0^+, T=2 state at 5.99 MeV in ^{28}Al was studied by Dickey et al. (Di 78) using the beta decay of ^{28}Mg. The ^{28}Mg was produced in the ^{26}Mg(^{18}O,^{16}O)^{28}Mg reaction. Since the β-decay half life was 21 hours it was possible to remove the ^{28}Mg from the beam and measure the branching ratio for the isospin-forbidden decay from the ^{28}Mg T=2 ground state to the 0^+, T=1 state at 0.97 MeV in ^{28}Al. M_{GT} for this transition is forbidden by angular momentum conservation. Dickey et al. used the measured branching ratio for the isospin-forbidden decay and the ft value for the isospin-allowed decays to compute the ft value for the isospin-forbidden decay. The isospin-forbidden Fermi matrix element is then computed from equation I.E-1 giving

$$ft = \frac{K}{G_V^2 M_F^2}$$

since $M_{GT} = 0$.

To calculate the isospin mixing from the value of M_F is a simple exercise. The ^{28}Mg parent state is a 0^+, T=2, T_z=-2 state. The final state in ^{28}Al at 0.97 MeV is mostly T=1, T_z=-1 with a small mixture of

the 5.99 MeV T=2, T_z=-1 analog state. Therefore, the states in ^{28}Al can be written as

$$|5.99\ \text{MeV}\rangle = -\alpha|1,-1\rangle + (1-\alpha^2)^{1/2}|2,-1\rangle$$

$$|.97\ \text{MeV}\rangle = (1-\alpha^2)^{1/2}|1,-1\rangle + \alpha|2,-1\rangle.$$

The ^{28}Mg ground state is related to the analog $|2,-1\rangle$ state by

$$T_+|^{28}\text{Mg(g.s.)},2,-2\rangle = (2(2+1)-(-2)(-2+1))^{1/2}|2,-1\rangle$$

$$= 2|2,-1\rangle$$

By definition

$$M_F = \langle .97|T_+|^{28}\text{Mg(g.s.)}\rangle$$

$$= [\alpha\langle 2,-1| + (1-\alpha)^{1/2}\langle 1,-1|]T_+|^{28}\text{Mg(g.s.)}\rangle$$

$$= 2\alpha$$

where the orthogonality of the $|1,-1\rangle$ and $|^{28}\text{Mg(g.s.)}\rangle$ states has been used. Writing the total Hamiltonian as $H = H_o + H_{CD}$, where all the charge-dependent terms are in H_{CD}, and treating H_{CD} as a perturbation we find in first order perturbation theory that the mixing amplitude is related to H_{CD} by

$$\alpha = \frac{\langle 5.99\text{Mev}|H_{CD}|.97\text{Mev}\rangle}{\Delta E}$$

where ΔE = 5.99 MeV - 0.97 MeV. For this decay Dickey et al. found $\langle H_{CD}\rangle = 17.0 \begin{smallmatrix} + 4.3 \\ - 5.8 \end{smallmatrix}$ keV. The measurement of $\langle H_{CD}\rangle$ for this decay was repeated by Alburger and Warburton using a different experimental method (Al 79). Alburger and Warburton determined that $\langle H_{CD}\rangle = 20.6 \pm 1.6$ keV.

The calculation of this charge-dependent matrix element did not require models of nuclear reactions or models to generate nuclear wave

functions. Beta decay is free of these complications, since the isospin raising and lowering operators do not change the space or spin part of the wave functions of the states involved in the decay. Measurement of the Fermi matrix element is the most direct measurement of isospin mixing in nuclei.

The ^{28}Al matrix element is much smaller than the matrix elements for ^{8}Be and ^{12}C, and one might wonder whether this is due to the difference between a rigorous (i.e. ^{28}Al) measurement and a model dependent (i.e. ^{8}Be and ^{12}C) calculation of the charge dependent matrix element. The small value of the ^{28}Al matrix element is easily explained in terms of the Coulomb force.

F. β-γ Circular Polarization Correlation Technique

While the ^{28}Mg β^- decay provided a very straightforward measurement of the isospin mixing in ^{28}Al, the mixing in this case was not expected to be particularly large. The relatively large energy difference (compared to ^{8}Be or ^{12}C) between the two 0^+ states suggest that these two states have differences other than their isospin quantum numbers. Any differences in the space or spin parts of their wave functions tend to reduce $\langle H_{CD} \rangle$ simply because the wave functions do not have a good overlap. As will be discussed below, the β^+ decay of ^{24}Al provides a situation where there are two 4^+ states of different T and where the energy difference is only 1.078 MeV, suggesting the possibility of two states very similar except for the isospin part of their wave functions. The problem with measuring M_F

in this case is that there is an allowed Gamow-Teller as well as the allowed Fermi transition to the states involved.

In this situation one must measure a quantity that depends on the interference of the Gamow-Teller and Fermi amplitudes as well as on the ft value. Defining the quantity y as

$$y = \frac{G_V M_F}{G_A M_{GT}} \qquad \text{I.F-1}$$

equation I.E-1 can be rewritten as

$$ft = \frac{K}{G_V^2 M_F^2} \quad \frac{y}{1+y^2} \qquad \text{I.F-2.}$$

Solving for M_F gives

$$|M_F| = ((K/G_V^2)/ft)\ y/(1+y^2)^{1/2}$$

For super-allowed T=1, $0^+ \rightarrow 0^+$ Fermi transitions, the ft value is given by (Ra 75)

$$ft = K/2G_V^2$$
$$= 3088.6 \pm 2.1 \text{ sec.}$$

Using this value

$$|M_F| = ((2ft(\text{super allowed})/ft(\text{case under study}))\ y/(1+y^2)^{1/2} \qquad \text{I.F-3.}$$

for a mixed Fermi and Gamow-Teller transition.

Now consider a $\beta^{\pm}$ transition from an initial state $|i\rangle = |J^{\pi},1,\pm1\rangle$ to a final state $|f\rangle$ in a $T_z = 0$ nucleus which is predominantly T = 0 with a T = 1 admixture. The final state can be written as

$$|f\rangle = (1-\alpha^2)^{1/2}|J^{\pi},0,0\rangle + \alpha|J^{\pi},1,0\rangle$$

where $|J^{\pi},0,0\rangle$ and $|J^{\pi},1,0\rangle$ are the eigenstates of the charge-independent part of the Hamiltonian. M_F is given by

$$M_F = \langle f|T_{\pm}|i\rangle = \alpha\sqrt{2}.$$

With all charge-dependent terms of the Hamiltonian in H_{CD} first-order perturbation theory gives

$$\alpha = \frac{\langle J^{\pi},1,0|H_{CD}|J^{\pi},0,0\rangle}{E_1 - E_0} \qquad \text{I.F-4}$$

If the sign of M_{GT} can be determined measurement of the ft value and y for a mixed transition of the form J^{π}, T=1 → J^{π}, T=0 yields M_F, α and $\langle H_{CD}\rangle$. For all the decays studied in this work the ft values are known, and the quantity y is determined using the β-γ circular polarization correlation.

For a $J(\beta)J'(\gamma)J''$ transition the β-γ circular polarization correlation function is (Ra 75)

$$W(\theta) = 1 + \tau(v/c)A\cos(\theta) \qquad \text{I.F-5}$$

where v/c = ratio of beta speed to the speed of light.

τ = +(-)1 for right(left) circularly polarized γ rays

θ = angle between the β and γ rays

$$A = (3^{1/2}/(6(1+y^2)))\,(((\mp J'(J'+1)-J(J+1)+2)/(J'(J'+1))^{1/2})+4y)$$

$$X\,(F_1(\lambda\lambda J''J') + 2\delta F_1(\lambda,\lambda+1,J''J') + \delta^2 F_1(\lambda+1,\lambda+1,J''J))/(1+\delta^2)$$

where the F coefficients, familiar from the theory of angular correlations, are tabulated in reference (Sc 66), δ is the γ ray mixing ratio and the +(-) sign refers to $\beta^{+(-)}$ decay.

Although the derivation of equation I.E-5 is rather tedious, the physics described by this equation is straightforward. In a pure Gamow-Teller decay of an unpolarized parent population the leptons carry away one unit of angular momentum. Conservation of angular

momentum demands that since the $\beta^{+(-)}$ particles are primarily right(left) handed the daughter nucleus have some net polarization with respect to the β direction. This polarization of the daughter nucleus is transferred to the γ rays emitted by the daughter, which implies different angular distributions for left-handed and right-handed γ rays (i.e. the polarization of the emitted γ rays varies with respect to the β direction).

In a pure Fermi decay of an unpolarized parent population the leptons carry away no angular momentum. Therefore, the daughter nuclei are unpolarized, and the distribution of right-handed and left-handed γ rays must be isotropic (i.e. there is no circular polarization of the γ rays).

If a decay has both Fermi and Gamow-Teller amplitudes, these amplitudes must be coherently added together to determine the daughter polarization. Neglecting for the moment the interference term the polarization of the daughter is the result of adding a polarized Gamow-Teller population to an unpolarized Fermi population. The result is a population with a polarization less than the pure Gamow-Teller daughter polarization. The reduction in the polarization will depend on the relative intensities of the two processes (i.e. the reduction will depend on the squares of the two amplitudes). The interference term which is proportional to the product of the Fermi and Gamow-Teller matrix elements can either increase or decrease the daughter polarization depending on the relative phases of the Gamow-Teller and Fermi amplitudes. The polarization of the daughter in a mixed transition is transferred to the γ rays emitted by the

daughter and produces a β-γ circular polarization correlation that depends on the interference of the Fermi and Gamow-Teller amplitudes.

The quantity A in equation I.F-5 is proportional to the polarization of the γ rays emitted by a beta decay daughter. For a pure Gamow-Teller decay, y=0, the polarization is calculated from the spin sequence and multipolarity of the γ ray. For a mixed transition the pure Gamow-Teller value of A is reduced by the factor $1/(1+y^2)$ which is just proportional to the ratio of the square of the Gamow-Teller matrix element to the sum of the squares of the Gamow-Teller and Fermi matrix elements. A also contains an additional interference term proportional to $y/(1+y^2)$ (i.e. the product of the Fermi and Gamow-Teller matrix elements).

G. Early β-γ Circular Polarization Experiments

In the mid sixites many nuclei were studied using the β-γ polarization correlation technique (Bl 62, Bl 64, Ha 63, Ma 65). At that time, state-of-the-art electronics permitted only the β branch with the highest end-point energy to be studied. The technique utilized β and γ detectors situated so that the average angle between the β's and γ's was 180°. Before being detected, the γ rays were analyzed by a reflection-type Compton polarimeter, which preferentially transmitted left-handed or right-handed γ rays depending on the orientation of the magnetic field in the polarimeter. The asymmetry in the count rate for the two possible orientations is proportional to the quantity A in equation I.F-5, from which y, M_F and

$\langle H_{CD} \rangle$ were calculated.

These early measurements were restricted to studying only the β branch with the highest end-point energy in a particular nucleus, because there was no technique for obtaining high count rates while maintaining energy resolution in the and β and ɣ energy spectra. With no energy spectra it was impossible to unfold different β branches from each other. The old experiments used a discriminator to eliminate all β's except β's from the highest end-point branch. Similarly, a ɣ-ray discriminator eliminated all low-energy ɣ rays that were not of interest. The β and ɣ signals that fired the discriminators in coincidence were then counted by scalers synchronized with the direction of the magnetic field in the polarimeter, and A was determined.

These experiments yielded good results for A (see Table I.G-1). However, the cases studied were ones where the isospin mixing was expected to be small, since the decays were always to the state of lowest possible excitation energy. Isospin mixing is expected to be large between states that are similar in all respects except for their total isospin (i.e. mixing is expected to be largest between the analog and anti-analog). The analog and anti-analog decays have similar end point-energies which generally do not correspond to the highest end-point energy possible. If the isospin symmetry is broken by the nuclear force the effects of the mixing produced by this breaking should be especially promenient in β decays to higher lying states close to the analog state.

TABLE I.G-1

SOME PREVIOUS β-γ CIRCULAR POLARIZATION CORRELATION RESULTS

(for the complete table see reference Ra 75)

Parent (decay)	A x 10^3	A x 10^3 if y=0	y x 10^3	$\lvert\langle H_{CD}\rangle\rvert$ (keV)
$^{20}F(\beta^-)$	174±14	167	-9±17	14^{+29}_{-14}
$^{24}Na(\beta^-)$	99±5	83	-21±7	5.4±2.2
$^{24}Al(\beta^+)$	-86±40	-83	4^{+46}_{-54}	$1.1^{+13}_{-1.1}$
$^{27}Mg(\beta^-)$	-221±19	-222	3^{+48}_{-51}	$3.6^{+57}_{-3.6}$
$^{41}Ar(\beta^-)$	75±8	95	27^{+10}_{-11}	20±8
$^{44}Sc(\beta^+)$	-127±14	-167	-48±17	16.6±6.3
$^{48}Sc(\beta^-)$	57±3	56	-2±4	$0.8^{+1.7}_{-0.8}$
$^{49}Ca(\beta^-)$	-132±17	-133	2±33	$1.3^{+21}_{-1.3}$
$^{52}Mn^m(\beta^+)$	-141±16	-167	-31±19	11±7
$^{57}Ni(\beta^+)$	71±11	133	-119±21	56±12
$^{58}Co(\beta^+)$	-167±3	-167	-3±4	$0.31^{+.40}_{-.33}$

H. Empirical Predictions for ^{24}Mg Isospin Mixing

^{24}Mg provides a case where the isospin mixing is expected to be large, and the mixing can be measured using the β-γ circular polarization correlation in the β^+ decay of ^{24}Al. The pertinent energy levels and β^+ decay branches are shown in figure I.H-1. The T=1 analog of the ^{24}Al ground state is a 4^+ state at 9.515 MeV (En 78). There are four other 4^+ states at lower excitation energies. Of these four other 4^+ states the state at 8.437 MeV has the largest ft value and as we shall see below contains a large piece of the anti-analog configuration of the ^{24}Al ground state. The large anti-analog configuration in the 8.437 MeV state makes the possibility of isospin mixing between this state and the analog state quite likely for any isospin symmetry breaking. Earlier experiments (Bl 64, Ha 63) were able to measure the the isospin mixing between the 9.515 MeV analog and the 4^+ state at 4.123 MeV using the β-γ circular polarization correlation. Using the β^+ decay of ^{24}Al the accepted result for the measured charge-dependent matrix element between these two states is $\langle H_{CD} \rangle = 1.1\ ^{+13}_{-1.1}$ keV (Ra 75). For the β^- decay of ^{24}Na the same $\langle H_{CD} \rangle = 5.4 \pm 2.2$ keV (Ra 75).

The size of $\langle 8.437 | H_{CD} | 9.515 \rangle$ matrix element can be estimated using the schematic model of McDonald and Adelberger (Mc 78). A schematic representation of the wave functions for several isospin multiplets is shown in figure I.H-2. These wave functions are suitable for any model with four-fold degenerate orbitals outside an ^{16}O core (e.g. the Nilsson model). The assumptions of the model (in

Figure I.H-1 The β^+ decay scheme of the ground state of ^{24}Al emphasizing the decays to 4^+ states.

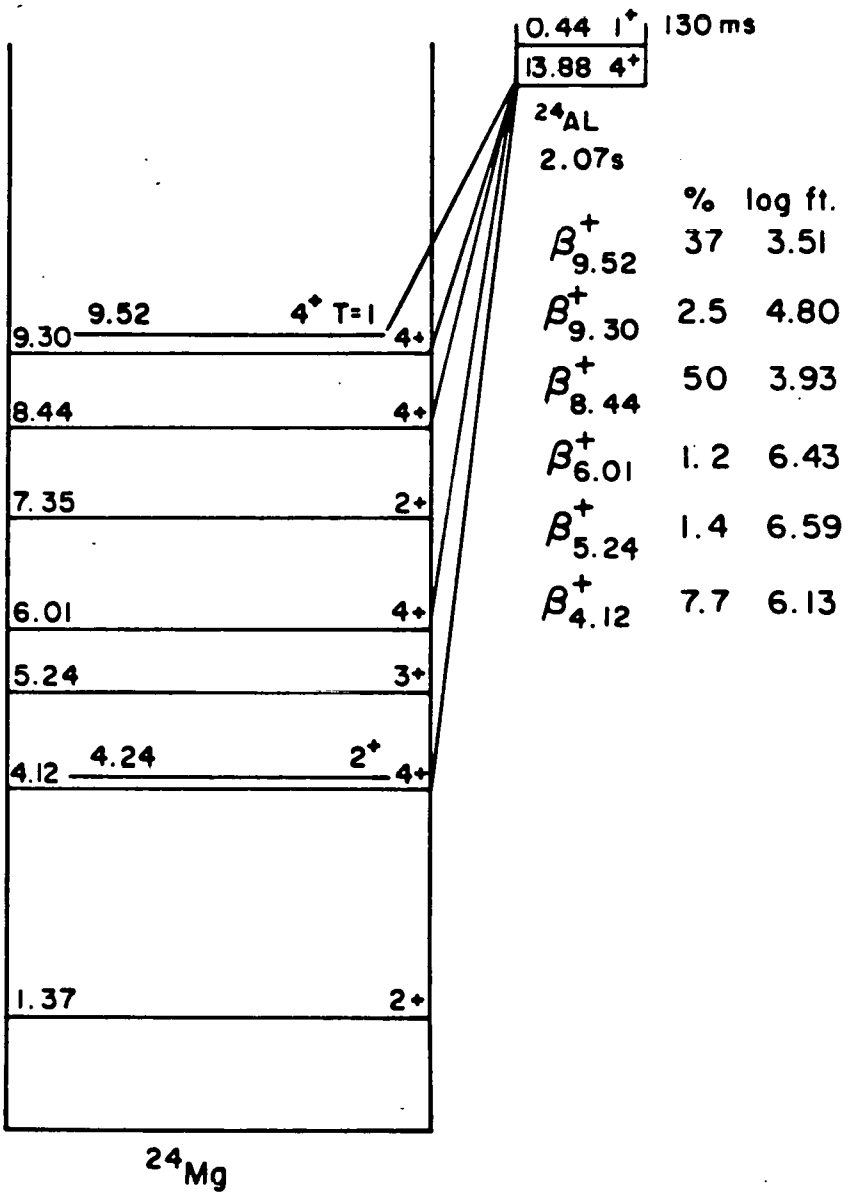
0.44 1+
130 ms
13.88 4+
24AL
2.07s
% log ft.
β+9.52 37 3.51
β+9.30 2.5 4.80
β+8.44 50 3.93
β+6.01 1.2 6.43
β+5.24 1.4 6.59
β+4.12 7.7 6.13
9.52
4+ T=1
9.30
4+
8.44
4+
7.35
2+
6.01
4+
5.24
3+
4.24
2+
4.12
4+
1.37
2+
24Mg

Figure I.H-2 Schematic wave functions for T=1 and T=1/2 states in A=22 through A=25 nuclei.

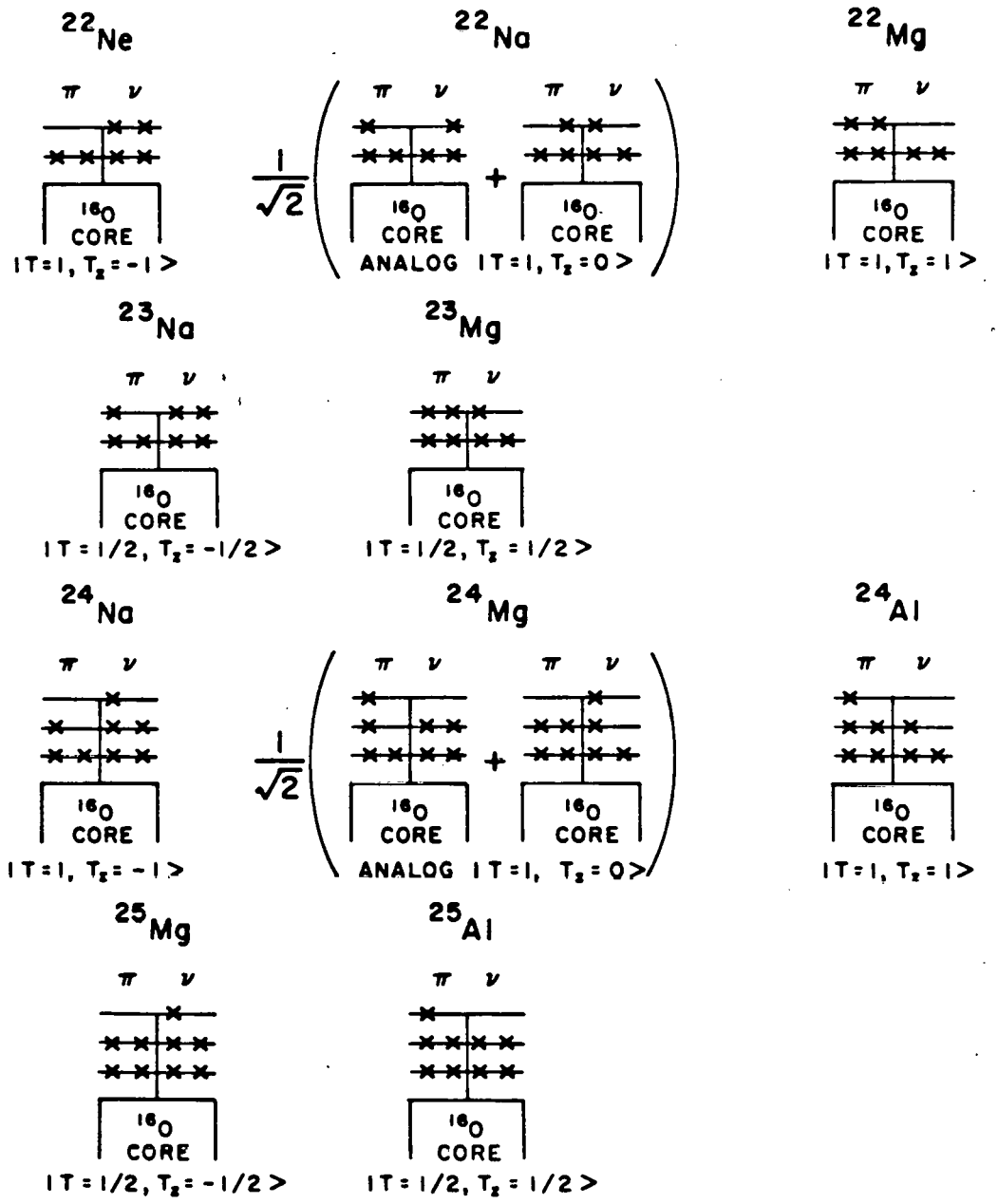
22Ne
22Na
22Mg
π ν
16O CORE
IT=1, Tz=-1>
1/√2
+
ANALOG IT=1, Tz=0>
IT=1, Tz=1>
23Na
23Mg
IT=1/2, Tz=-1/2>
IT=1/2, Tz=1/2>
24Na
24Mg
24Al
IT=1, Tz=-1>
ANALOG IT=1, Tz=0>
IT=1, Tz=1>
25Mg
25Al
IT=1/2, Tz=-1/2>
IT=1/2, Tz=1/2>

addition to the "idiot model" wave functions) are that the isospin mixing is due only to Coulomb interactions and that the mass differences in an isospin multiplet are due solely to the two body Coulomb interactions of the valence protons plus differences in the single particle energies of neutrons and protons. The diagonal matrix elements of the charge-dependent term of the Hamiltonian can then be expressed in terms of the mass differences of the members of an isospin multiplet.

In ^{24}Na there is one valence proton outside the ^{20}Ne ground state. Therefore, there is only one valence-proton, charge-dependent matrix element, which will be denoted by C(1). In ^{24}Al there are two valence protons in the first valence orbital and one valence proton in the second valence orbital giving a mass splitting

$$\text{MASS}(^{24}\text{Al})-\text{MASS}(^{24}\text{Na}) = 2C(1)+C(2)+2C(12)+C(11)$$

where C(2) is the matrix element for the interaction of a proton in the second valence orbital with the the ^{20}Ne ground state, C(11) is the matrix element for the interaction of two protons in the first valence orbital and C(12) is the matrix element for the interaction of a proton in the first valence orbital with a proton in the second valence orbital. For the ^{24}Mg analog state, a similar procedure gives

$$\langle H_{CD} \rangle = 1/2(C(1)+C(2)+C(12)+2C(1)+C(11)).$$

This implies that

$$\text{MASS}(^{24}\text{Al})+\text{MASS}(^{24}\text{Na})-2\text{MASS}(^{24}\text{Mg(9.515 MeV)})$$

$$= 2C(1)+C(2)+2C(12)+C(11)+C(1)-(C(1)+C(2)+C(12)+2C(1)+C(11))$$

$$= C(12)$$

$$= 5513+13879-2(9515) \text{ keV}$$

= 362 keV

where the energies used are from reference En 78.

To solve for the rest of the C's consider the ground states of ^{25}Al and ^{25}Mg. These two ground states give

MASS(^{25}Al)-MASS(^{25}Mg)

= C(2)+2C(12)+2C(1)+C(11)-(2C(1)+C(11))

= C(2)+2C(12)

= C(2)+.724 keV

= 4278 keV

implying

C(2) = 3554 keV

The A=22 nuclei give

MASS(^{22}Ne)+MASS(^{22}Mg)-(^{22}Na(657))

= 2C(1)+C(11)-2C(1)

= C(11)

= 634 keV

And the ^{23}Mg and ^{23}Na ground states give

MASS(^{23}Mg)-MASS(^{23}Na) = C(1)+C(11)

= C(1) + 634 keV

= 4069 keV

implying

C(1) = 3435 keV

Now the off-diagonal matrix element in ^{24}Mg given by $\langle$anti-analog$|H_{CD}|$analog$\rangle$ is easily calculated from the C's. The schematic anti-analog state in this model is just the schematic state for ^{24}Mg in figure I.H-2 with the + sign changed to a - sign. This

sign change makes the cross terms cancel in the matrix element giving

$$\langle \text{anti-analog} | H_{CD} | \text{analog} \rangle = 1/2(C(1)+C(2)+C(12)-2C(1)-C(11))$$

$$= 1/2(3435 + 3554 + 362 - 2(3435) - 634) \text{ keV}$$

$$= -77 \text{ keV}$$

This empirical estimate of the size of the $\langle 8437 | H_{CD} | 9515 \rangle$ matrix element in ^{24}Mg assumes that the 8437 keV state is the anti-analog of the 9515 keV state. A nuclear model prediction of $\langle H_{CD} \rangle$ is necessary to determine whether or not this value of $\langle H_{CD} \rangle$ can be accounted for by the Coulomb force alone or whether a charge dependent nuclear force is necessary to obtain this value.

It is interesting to test the general validity of the above model by examining its predictions for the well studied cases of ^{8}Be and ^{12}C. The model predicts charge dependent matrix elements of 140 keV and 125 keV for ^{8}Be and ^{12}C respectively. These matrix elements should be compared with the measured values of 143 keV and 110 ± 30 keV. The agreement is excellent.

I. Nilsson Model Predictions

The collective motion of ^{24}Mg has been extensively studied and many of the observed properties of ^{24}Mg are explained by collective models (Wa 81, En 78 and references therein). A basic, although not entirely satisfactory, understanding of the nuclear structure of ^{24}Mg can be obtained by applying the Nilsson model (Ni 55) in the asymptotic limit to ^{24}Mg. In this limit ^{24}Mg is pictured as consisting of a deformed ^{20}Ne core with four nucleons outside the

core. Using this model the log(ft) values for the β^+ decays of ^{24}Al to the analog and anti-analog states in ^{24}Mg have been calculated (Bl 81).

The calculation was done by first considering the 4^+, T=1 ^{24}Al ground state, shown schematically in figure I.H-2. In this model the valence nucleons are in the $d_{5/2}$ shell. The lowest orbital outside the ^{16}O core has $|\underline{\Omega}|=1/2$, the next higher orbital has $|\underline{\Omega}|=3/2$ and the third orbital has $|\underline{\Omega}|=5/2$ where $\underline{\Omega}$ is the projection of the particle angular momentum along the axis of symmetry of the nucleus and is a good quantum number. In ^{25}Al the lowest orbital is filled to produce the ^{20}Ne core. The second orbital is filled except for a neutron missing from the $\underline{\Omega}=-3/2$ orbital. The final proton is in the $\underline{\Omega}=5/2$ orbital. The 5/2 proton and the -3/2 neutron hole are then coupled to a total projection of 4 to give the observed 4^+ ground state of ^{24}Al with total $\underline{\Omega}=K=4$ where K is the total angular momentum (i.e core plus valence angular momentum) projection on the core axis of symmetry. The state vector for the valence nucleons can then be written as

$$|p_{5/2}(1),p_{3/2}(2),p_{-3/2}(3),n_{3/2}(4)\rangle$$

where the (i) stand for the coordinates of particle i, the p and n refer to whether the particle is a proton or neutron and the angular dependence of the $\underline{\Omega}=5/2,3/2$ and -3/2 wave functions is given by $Y_2^2\alpha$, $Y_2^1\alpha$ and $Y_2^{-1}\beta$ respectively. The Y's, α and β are the usual spherical harmonics and spin wave functions. The analog state is obtained by applying the isospin lowering operator given by $T_- = \sum_i \tau_{-i}$ where i is

summed over the four valence nucleons. This gives the analog state as the sum

$$|p_{5/2}(1),p_{3/2}(2),p_{-3/2}(3),n_{3/2}(4)\rangle/\sqrt{2}$$

plus

$$|p_{5/2}(1),p_{3/2}(2),p_{-3/2}(3),n_{3/2}(4)\rangle/\sqrt{2}$$

The anti-analog state is given by the difference instead of the sum of the above states.

To calculate the ft value for the analog decay of ^{24}Al, one needs the Fermi and Gamow-Teller matrix elements. The Fermi matrix element is trivially given by $\langle \text{analog}|T_-|\text{parent}\rangle = \sqrt{2}$. For the Gamow-Teller matrix element the terms that produce non-zero contributions are terms involving

$$\tau_{-i}\sigma_{zi}|\underline{Q}=5/2\rangle=|\underline{Q}=5/2\rangle$$

and

$$\tau_{-i}\sigma_{zi}|\underline{Q}=-3/2\rangle\approx Y_2^{-1}\sigma_z\beta= -Y_2^{-1}\beta.$$

With the sign change of the second term the first and second terms cancel each other in the overlap giving $M_{GT}\approx 0$. The log(ft) value is then given by

$$\log ft = \log(K/G_V^2M_F^2) = 3.49.$$

This agrees well with the measured log(ft) = 3.510 ± 0.018 (Wa 81) of the analog decay. The Nilsson model correctly predicts the inhibition of the Gamow-Teller decay to the analog state.

For the log(ft) value of the β^+ decay to the anti-analog state

the same Gamow-Teller operator is applied to the same initial state as was done for the analog decay. Now the final state is the anti-analog state which has the relative - sign instead of the + sign. In this case instead of terms cancelling, as was the case for the analog decay, the terms are both negative, giving

$$\langle \text{anti-analog} | \sum_i \sigma_{zi} \tau_i | ^{24}\text{Al ground state} \rangle = (-1-1)/\sqrt{2} = -\sqrt{2}.$$

This matrix element is related to the standard M_{GT} by multiplication by the (4,1,4,0|4,4) vector coupling coefficient, since the parent and daughter state have both J=4 and K=4, and σ_z is the 0 component of a vector operator in spin-orbit space. This gives $M_{GT} = -(8/5)^{1/2}$.

Assuming M_F=0 for this decay and substituting in equation I.E-1 gives a log(ft) = 3.39 for the anti-analog decay. Excepting the analog decay the smallest observed log(ft) is for the decay to the 4^+ state at 8.437 MeV. The observed log(ft) is 3.93 ± 0.02 (Wa 81). The transition rate is approximately three times slower than predicted for the pure anti-analog transition. Since there are no other observed decays with a log(ft)<4, it seems likely that the 8.437 MeV state contains more anti-analog configuration than any other state accessible by beta decay. The large B(E2)(~11W.U.) measured by Wharburton et al. (Wa 81) for the 8.437 MeV, 4^+(K=4) → 7.35 MeV, 4^+(K=0) γ-ray transition suggests the possibility of strong interband mixing of the K=4 and K=0 bands. A mixing of this sort would tend to produce a larger log(ft) for the transition to the 8.437 MeV state by mixing some non anti-analog (beta-decay forbidden) configuration into

the 8.437 MeV state. Where the rest of the anti-analog configuration has gone is still a mystery since there are no other strong beta transitions. This quenching of the Gamow-Teller strength is a general problem. One explanation of this quenching involves Δ excitations (Bl 81).

Assuming for the moment that the 8.437 MeV state is an anti-analog state the $\langle$anti-analog$|H_C|$analog$\rangle$ matrix element can be written as

$$\langle\text{anti-analog}|H_{C,SP}|\text{analog}\rangle + \langle\text{anti-analog}|H_{C,V}|\text{analog}\rangle$$

where H_C is the total Coulomb interaction, $H_{C,SP}$ is the Coulomb interaction of the valence protons with the ^{20}Ne core and $H_{C,V}$ is the Coulomb interaction of the valence protons with each other. Using the determinant wavefunctions given above,

$$\langle H_{C,V}\rangle = (e^2/2) \int (1/r_{12}) d^3r_1 d^3r_2 \; (|p_{3/2}(1)|^2 |p_{5/2}(2)|^2 - |p_{3/2}(1)|^2 |p_{3/2}(2)|^2 - (p^*_{3/2}(1) p_{5/2}(1) p_{3/2}(2) p^*_{5/2}(2))$$

where r_{12} is the magnitude of the separation between particle 1 and particle 2 and the exchange term for the 3/2,-3/2 configuration is zero due to the orthogonality of the spin wave functions. To evaluate this matrix element the usual expansion of $1/r_{12}$ in spherical harmonics is made. Since all the wave functions involved contain a spherical harmonic with L=2, only the terms in the expansion with

L=0,2 or 4 will be non-zero. Assuming identical radial wave functions for all the orbitals the L=0 term of the expansion gives zero, since the direct terms will cancel and the exchange term will be zero by orthogonality of the spherical harmonics. The terms to be evaluated are

$$\langle H_{C,V,L}\rangle = -e^2/2(\zeta_{rad,L})(2,0,2,0|L,0)^2\{(2,1,2,-1|L,0)(2,2,2,-2|L,0) + (2,1,2,-1|L,0)(2,-1,2,1,|L,0) + (2,-1,2,2,|L,1,)(2,1,2,-2,|L,-1)\}$$

where

$$\zeta_{rad,L} = \int_0^\infty dr_1 r_1^2 R(r_1)\{\int_0^{r_1} dr_2 r_2^2 (r_2^L/r_1^{L+1}) R(r_2) + \int_{r_1}^\infty dr_2 r_2^2 (r_1^L/r_2^{L+1}) R(r_2)\}$$

and R(r) is the radial wave function.

Estimating $\zeta_{rad,L} \approx 1/(2R)$ where R is the nuclear radius given by $R = 1.2 \text{ fm}(24)^{1/3} = 3.5$ fm gives

$$\langle H_{C,V,L=2}\rangle \approx (-9/49)(1.44 \text{ MeV-fm}/4(3.5 \text{ fm})) \approx -20 \text{ keV}$$

$$\langle H_{C,V,L=4}\rangle \approx (-25/441)(1.44 \text{ MeV-fm}/4(3.5 \text{ fm})) \approx -5 \text{ keV}$$

giving a total $\langle H_{C,V}\rangle \approx -25$ keV.

A reliable estimate of $\langle H_{C,SP}\rangle$ is a difficult theoretical problem. To calculate this matrix element one must have orbitals that are consistent with the binding energies of the valence nucleons and the nonspherical charge distribution of the ^{20}Ne core. These calculations have not been done.

In the empirical calculation the two body interactions of the valence nucleons contributed C(12)-C(11)=1/2(362-634) keV=-141 keV to

the $\langle$anti-analog$|H_{CD}|$analog$\rangle$ matrix element. In the Nilsson model calculation the valence nucleons contribute only -25 keV to the same matrix element when only the Coulomb interaction is considered. The much larger negative value of the empirical calculation results from the relatively large value of C(11) compared to C(12). One possible explanation of this difference is the existence of a short range (i.e. nuclear) charge-dependent interaction. This type of interaction would tend to increase C(11) since C(11) is the matrix element for two protons in the same orbital but not change C(12) since C(12) is the matrix element for protons in different orbitals. The different orbitals have a small overlap so that the contribution of the short range interaction tends to be small.

While none of the Nilsson model arguments are rigorous enough to definitely confirm or deny the existence of a charge-dependent nuclear force mixing T=1 and T=0 states in ^{24}Mg the indications are that a charge-dependent matrix element of -77 keV will be difficult to obtain with the Coulomb force alone. If there is interband mixing, which is one possibility that could lead to a better prediction of the log(ft) for the decay to the 8.437 MeV state and for some of the observed β decay strengths, the value of the Coulomb matrix element calculated in the Nilsson model would probably decrease. The decrease would result from other T=0 spatial and spin configurations being mixed with the anti-analog configuration to produce the 8.437 MeV state. With this suggestion of possible large isospin symmetry breaking in ^{24}Mg a particularly clean measurement of the actual isospin mixing was carried out.

CHAPTER II

EXPERIMENTAL TECHNIQUE

A. Introduction

The experimental quantity of interest is the asymmetry A in the β-γ circular polarization correlation function given in equation I.F-5 by $W = 1 + \tau(v/c)A\cos(\theta)$. To determine A one needs to measure the relative number of right-handed and left-handed γ rays emitted into a solid angle $\Delta\Omega$ in the θ direction. The number of right-handed γ rays is proportional to $N_{Ro} = 1 + \langle v/c\rangle A\langle\cos(\theta)\rangle$ and the number of left-handed γ rays is proportional to $N_{Lo} = 1 - \langle v/c\rangle A\langle\cos(\theta)\rangle$ where $\langle v/c\rangle$ indicates that v/c has been averaged over the β spectrum and $\langle\cos(\theta)\rangle$ indicates that $\cos(\theta)$ has been averaged over the solid angle of the detection system. Therefore,

$$A = \frac{N_{Ro} - N_{Lo}}{N_{Ro} + N_{Lo}} \frac{1}{\langle v/c\rangle\langle\cos(\theta)\rangle}. \qquad \text{II.A-1}$$

B. Rabbit Target Transport System

The half life for the β^+ decay of ^{24}Al is 2.07 seconds. Therefore a system that continually produces ^{24}Al is required to study the ^{24}Al β^+ decay. The rabbit target transport system is a pneumatic system that shuttles a target between the beam, where the radioactive isotopes are produced, and a counting station where experiments are conducted. The counting station and beam are separated by a concrete

shielding wall to keep background produced by the beam out of experiments.

The rabbit system consists of a section of 10 cm beam tube with a 1.25 cm square rabbit tube inserted perpendicular to the beam axis (see figure II.B-1). The square rabbit tube has 6.4 micron Havar (Havar is a product of Hamilton Technology, Inc.) entrance and exit foils for the beam. The beam is collimated by a 1.6 mm Ta aperture, passes through the entrance foil, the target, and the exit foil and stops in a Faraday cup. After the target has been irradiated it is shuttled on a rabbit to the counting station by opening a solenoid valve that lets pressurized air into the rabbit tube. The pressurized air is stored in a reservoir with adjustable pressure and flow. The pressure and flow into the reservoir are set by a regulator and needle valve so that a high-pressure kick is given to the rabbit. The flow through the needle valve is low enough so that as the air expands into the rabbit tube the pressure drops and the rabbit slows down as it approaches the counting position, minimizing the shock to the target as the rabbit stops. After the counting period is over, another solenoid valve with a similar reservoir opens and evacuates the rabbit tube. With the rabbit tube evacuated atmospheric pressure pushes the rabbit back into the beam and the cycle begins again.

The timing of the rabbit cycle is controlled by a solid-state timer box. The timer box has an adjustable cycle length and eight TTL level outputs that are independently on for any period during the cycle. Two of the TTL outputs drive optically isolated relays that open the solenoid valves. The independent adjustment of the on time

Figure II.B-1 Schematic diagram of Rabbit Target Transport System.

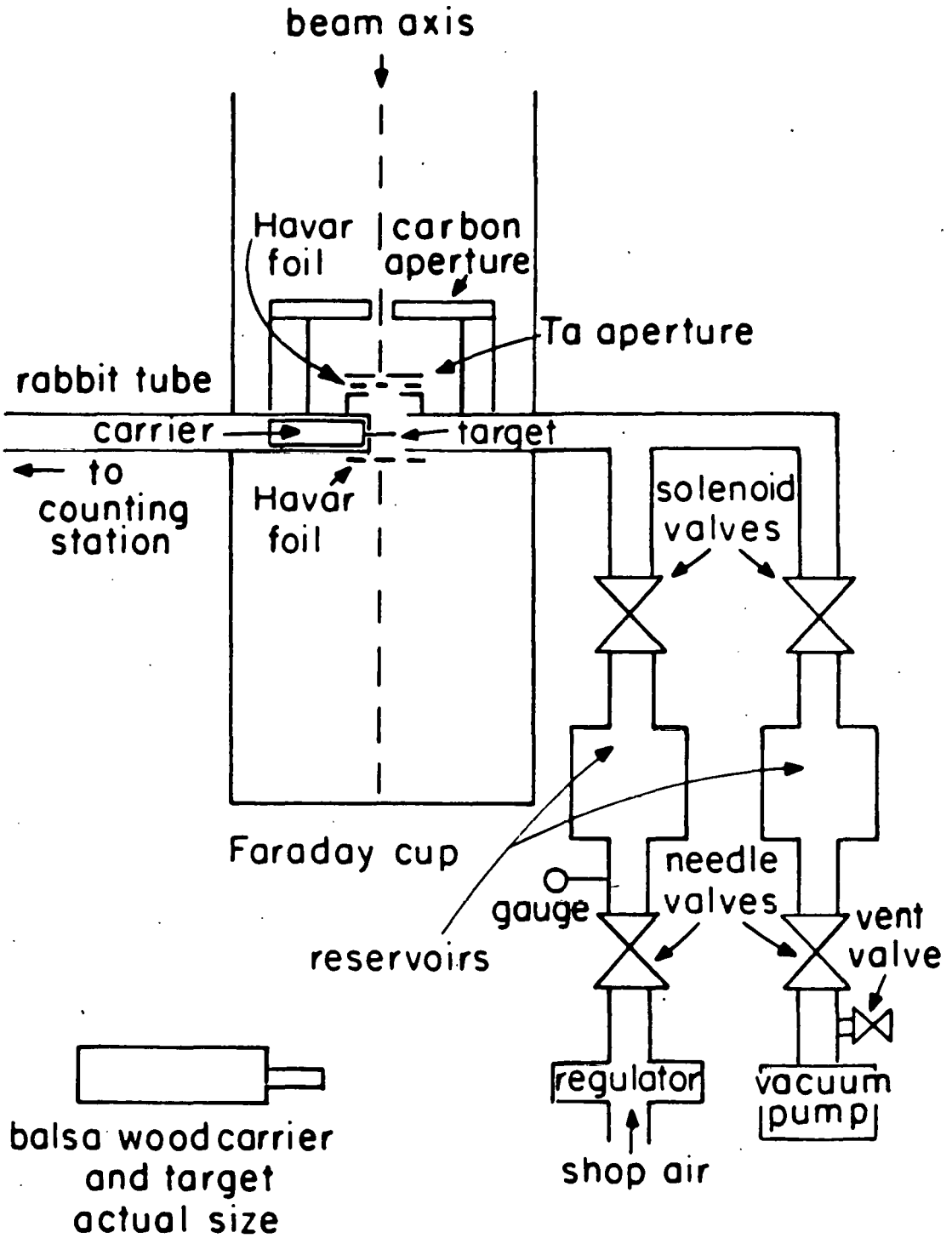
beam axis
Havar foil
carbon aperture
Ta aperture
rabbit tube
carrier
target
to counting station
Havar foil
solenoid valves
Faraday cup
needle valves
gauge
vent valve
reservoirs
regulator
vacuum pump
shop air
balsa wood carrier and target actual size

of the TTL levels allows the time the target is in the beam, the time the target is at the counting station and the time the target is in transit to be independently set. With this scheme the lower limit on the transit time from the beam to the counting station is approximately 0.1 sec.

The targets used in the rabbit are mounted on balsa wood carriers. The carriers are 3.2 cm by 1 cm by 1 cm pieces of balsa wood (see figure II.B-1). Any solid material can be directly epoxied to the carrier or mounted on a backing that can be epoxied to the carrier.

C. Polarimeter

The circular polarization of the γ rays is measured with a Compton transmission polarimeter. The polarimeter (developed at Chalk River for the Mark II ^{21}Ne parity mixing experiment) has a Hyperco core 10.2 cm long and 7.3 cm in diameter. A copper winding is wrapped around the core and the wrapped core is enclosed in an iron flux return (see figure II.C-1). When the coil saturates the magnetization of the core the two unpaired electrons in each iron atom have their spins aligned opposite to the magnetic field in the core.

The Compton scattering cross section for circularly polarized γ rays on polarized electrons has both a spin-independent term (the usual Klien-Nishina cross section) and a spin-dependent term. The spin-dependent term depends on the helicity of the γ ray and the relative orientation of the γ-ray and electron spins. It has been

Figure II.C-1 Scale drawing of the β-γ circular polarization correlation detection apparatus.

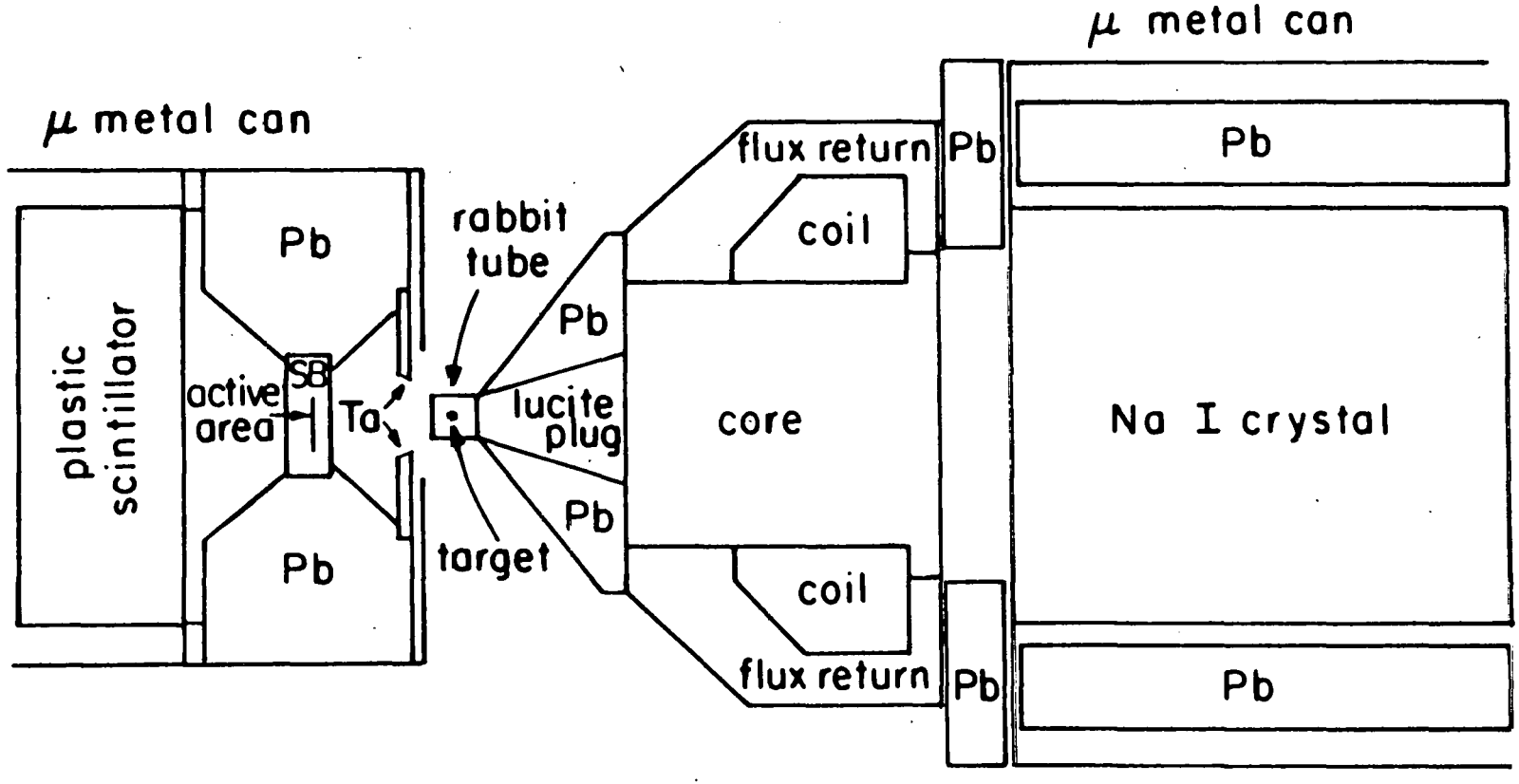
μ metal can
μ metal can
plastic scintillator
Pb
active area
SB
Ta
rabbit tube
target
Pb
lucite plug
Pb
flux return
coil
Pb
core
coil
flux return
Pb
Pb
Na I crystal
Pb

shown (Ch 65) that for a magnetized iron core right-handed γ rays are preferentially transmitted with no loss of energy due to scattering when the magnetic field in the core is anti-parallel to the γ-ray momentum. Similarly, left handed γ rays are preferentially transmitted with no energy loss when the magnetic field in the core is parallel to the γ-ray momentum. For right handed γ rays

$$N_R \propto N_{Ro} e^{-(\sigma \mp \sigma_s)x}$$

where

N_R = the number of transmitted full energy right-handed γ rays

N_{Ro} = the number of incident full energy right-handed γ rays

x = length characteristic of the polarimeter

$\sigma \propto$ the spin-independent Compton cross section

$\sigma_s \propto$ the spin-dependent Compton cross section

and the upper(lower) sign is used for the magnetic field parallel(anti-parallel) to the γ-ray momentum. For left-handed γ rays

$$N_L \propto N_{Lo} e^{-(\sigma \pm \sigma_s)x}$$

where

N_L = the number of transmitted full energy left-handed γ rays

N_{Lo} = the number of incident full energy left-handed γ rays

and the upper(lower) sign applies as above.

The efficiency of the polarimeter, η, is defined by

$$\eta = (N_{R+} - N_{R-})/(N_{R+} + N_{R-}) = -(N_{L+} - N_{L-})/(N_{L+} + N_{L-})$$

where

N_{R+} = the number of right handed γ rays transmitted with momentum anti-parallel to the magnetic field

N_{R-} = the number of right handed γ rays transmitted with momentum parallel to the magnetic field

N_{L+} = the number of left handed γ rays transmitted with momentum anti-parallel to the magnetic field

N_{L-} = the number of left handed γ rays transmitted with momentum parallel to the magnetic field

and it is assumed that the incident γ rays are totally right(left) circularly polarized for the expression containing the R(L) subscripts.

For incident γ rays of arbitrary polarization P,

$$P = (N_{Ro} - N_{Lo})/(N_{Ro} + N_{Lo}).$$

Now the polarization of the incident γ rays can be determined from η and the difference in count rate through the polarimeter for the two direction of the magnetic field. The pertinent quantity is

$$\frac{N_+ - N_-}{N_+ + N_-} = \frac{N_{R+} + N_{L+} - N_{R-} - N_{L-}}{N_{R+} + N_{L+} + N_{R-} + N_{L-}}$$

where

N_+ = total number of γ rays transmitted for γ-ray momentum anti-parallel to the magnetic field

N_- = total number of γ rays transmitted for γ-ray momentum parallel to the magnetic field.

A little algebra gives

$$\frac{N_+ - N_-}{N_+ + N_-} = \eta \frac{(N_{R+} + N_{R-}) - (N_{L+} + N_{L-})}{(N_{R+} + N_{R-}) + (N_{L+} + N_{L-})} .$$

Now $(N_{R+} + N_{R-}) \propto N_{Ro}e^{-\sigma x}\cosh(\sigma_s x)$ and $(N_{L+} + N_{L-}) \propto N_{Lo}e^{-\sigma x}\cosh(\sigma_s x)$. This implies

$$(N_+ - N_-)/(N_+ + N_-) = \eta(N_{Ro} - N_{Lo})/(N_{Ro} + N_{Lo}) = \eta P$$

which relates the polarization of the incident γ rays to the measured asymmetry of transmitted full energy γ rays for the two directions of the magnetic field in the polarimeter. Using this result equation II.A-1 can be rewritten in terms of the number of γ rays transmitted through the polarimeter as

$$A = \frac{N_+ - N_-}{N_+ + N_-} \frac{1}{\eta \langle v/c \rangle \langle \cos(\theta) \rangle} .$$

The value of η depends on the geometry of the core, the magnetization of the core and the incident γ-ray energy. The dependence of η on the γ-ray energy is calculated from the energy

dependence of the Compton cross section (Ch 65). None of the other factors that determine η depend on the γ energy; therefore, only one measurement of η is necessary to normalize the functional dependence of η on γ-ray energy. The normalization for the polarimeter was done by measuring η for the 2.754 Mev γ rays from the $^{24}Na(\beta^-)^{24}Mg^*(4.214\ Mev)(\gamma)^{24}Mg^*(1.369\ Mev)$ decay sequence (Vl 81). The measured value of η for the 2.754 Mev γ ray (Vl 81) is 0.03497 $\mp$0.00083. The γ-ray energies and corresponding values of η, normalized to the above measurement and of interest in this work, are listed in table II.C-1.

The current to the polarimeter is controlled by a flipping bridge. With the flipping bridge pot the adjustable range of the current to the polarimeter is 0 to 4.5 amps. The bridge allows the direction of the magnetic field in the core to be flipped manually or by an external TTL signal. In addition to the coil used to magnetize the core, the polarimeter has a sense coil around the core. The output of the sense coil is fed to an integrator in the flipping bridge. The output of this integrator is proportional to the magnetic field in the core. The integrator output is fed to a level shifter; the level shifter output is always a positive voltage proportional to the magnetic field in the core.

The flipping times and integrator outputs were measured over the entire range of magnet currents. The integrator output , via the level shifter, was fed to a ND2400 multichannel analyzer operated in the LIST mode. A BNC model DB-2 Random Pulse Generator, operated in the 1 kHz REP mode, supplied an input to an ORTEC model 416A Gate and

TABLE II.C-1

POLARIMETER EFFICIENCIES

γ Ray Energy	Efficiency(η)
1.778 Mev	0.03090±0.00073
2.754 Mev	0.03497±0.00083
7.068 Mev	0.03054±0.00072

Delay Generator the output from which supplied the DC strobe input to the ND2400. Each time a DC strobe was supplied, the ND2400 converted the integrator output level and stored the result in the next channel. The time per channel was calibrated by scaling the 416A output for 10 seconds to obtain the time per channel. In this fashion, a plot of integrator output vs. time was obtained. The flipping time and change in integrator outputs for both the + to - and - to + transitions for a given current were then averaged. Table II.C-2 contains polarimeter currents, change in integrator outputs and flipping times for different magnet currents. The β-γ circular polarization correlation experiments were done with a 2.5 amp magnet current. The 2.5 amp current was chosen since a higher current would mainly increase the stray fields outside the core and not significantly increase the magnetization in the core. The larger flipping time, compared to that which results from the 4.5 amp current used in the parity violation experiment and the efficiency measurement, is of no consequence in a rabbit experiment since the magnet current is always flipped while the target is being bombarded.

A conical Pb collimator was mounted on the polarimeter to define the solid angle subtended by the polarimeter (see figure II.C-1). The tapered hole in the collimator was fitted with a lucite plug. Due to its low Z, the lucite plug stops betas with a minimum amount of bremsstrahlung reducing the background produced by the betas in the γ detector.

TABLE II.C-2

POLARIMETER PARAMETERS

Bridge pot	polarimeter current	flip time	change in integrator output (i.e. $\Delta\vec{B}$)
1.43	4.5 Amps	340 msec	2504 channels
1.27	4.0 Amps	372 msec	2496 channels
1.10	3.5 Amps	426 msec	2486 channels
0.95	3.0 Amps	473 msec	2472 channels
0.78	2.5 Amps	575 msec	2460 channels
0.63	2.0 Amps	696 msec	2440 channels
0.46	1.5 Amps	951 msec	2412 channels
0.31	1.0 Amps	1440 msec	2356 channels
0.23	.75 Amps	1970 msec	2296 channels

D. NaI Detector

After being analyzed by the polarimeter the γ rays were detected with a 5 x 6 NaI crystal and a RCA model 4900 7.5 cm phototube. The NaI crystal was mounted in a cylindrical Pb shield assembly. The whole NaI-phototube-Pb shield assembly was then mounted in a μ-metal shield which shields the phototube from the magnetic field produced by the polarimeter. An additional doughnut shaped piece of Pb shielding was mounted on the μ-metal shield to define the solid angle subtended by the NaI crystal (see figure II.C-1).

The change in the axial magnetic field inside the μ-metal shield was measured with a Hall probe as the polarimeter magnetic field was flipped between the two possible axial orientations with a 2.5 amp current. The variation in the magnetic field at the position of the phototube was 0.05 gauss (i.e. $\mp$ 0.025 gauss). With this small magnetic field the gains in the NaI spectra for the two states of the polarimeter differed by a factor of only 0.0001.

E. Beta Telescope

The betas were detected in a telescope consisting of a totally depleted silicon surface barrier detector that generates the ΔE signal and a cylindrical plastic scintillator that generates the E signal. The surface barrier detector is an ORTEC model TB-18-300-700 with an active area of 300 mm^2 and a sensitive depth of 700 microns. The surface barrier detector was used to generate the ΔE signal since an

energetic γ ray has a very small probability of generating a signal in silicon. The plastic scintillator is a cylinder 12.5 cm in diameter and 5 cm thick coupled to a RCA model 4522 12.5 cm phototube with a 2.5 cm section of light pipe.

The surface barrier detector was mounted in a combination Pb and Ta shield (see figure II.C-1). The shield performs two functions. It collimates the betas, and it shields the plastic from many cascade γ rays that could sum with the betas in the plastic. The plastic, phototube and surface barrier detector with shield are all enclosed in a μ-metal can to shield the phototube and betas from the magnetic field produced by the polarimeter. The μ-metal can has a 3.75 cm entrance hole for the betas. With the polarimeter flipping with a 2.5 amp current the variation in the axial magnetic field at the counting position of the target was 35 gauss. At the entrance hole in the μ-metal can, approximately 1 cm closer to the telescope, the variation in the axial magnetic field was 18.5 gauss. At the position of the surface barrier detector the variation was 0.78 gauss. And at the position of the plastic phototube the variation was 0.06 gauss. Without the μ-metal shield the count rates for betas detected with a surface barrier-plastic coincidence (see section F for details of the electronics) differed by 1-2% for the two states of the polarimeter. With the μ-metal shield in place the two rates differed by approximately 0.05% for the steadiest beams.

The effect of the Pb and Ta shield was determined by measuring the ratio of events that produced coincidences in the surface barrier and plastic detectors to the total number of surface barrier events

(details of the electronics used for the measurement are given in section F). With the shield removed this ratio was 25% for both the β^- and β^+ particles emitted by ^{24}Al and ^{28}Al. With the shield in place this ratio was 50% showing that the shield prevented many scattered betas from reaching the plastic.

The γ-ray rejection efficiency of the telescope was measured with a ^{22}Na source. The γ rays were detected in the plastic with a coincidence required between the surface barrier and plastic signals (see section F for details of the electronics). Data were then taken for an equal amount of live time with no coincidence requirement. The ratio of the number of γ rays detected with the coincidence requirement to the number of γ rays detected without the coincidence requirement was 0.0015 ∓ 0.0001.

The absolute γ-ray efficiency was measured with a calibrated ^{137}Cs source. The ^{137}Cs source was placed at the target counting position and γ rays were detected in the plastic with no coincidence requirement. The ^{137}Cs source was last calibrated on February 1, 1976. At that time the activity was 11.36 μC. Using $A = A_o(.5)^{t/t_{1/2}}$ with $t_{1/2} = 30.17$ years and $t = 5.40$ years for June 24, 1981, the date of the measurement, $A = 11.36(.5)^{.179} = 10.04$ μC. The total number of γ rays detected by the plastic in 184 live seconds was 1219687, yielding an average rate of 0.179 ∓ 0.002 μC. This gives an absolute efficiency of 0.01782 ∓ 0.00002.

The plastic energy scale was calibrated using ^{22}Na, ^{24}Na and ^{137}Cs γ-ray sources. Data were acquired for all sources with no coincidence requirement. A 50 ohm attenuator was always used to keep

the plastic signals from being too large for the ADC used. For the ^{24}Na and ^{137}Cs sources data were acquired with attenuator settings of 2 and $\sqrt{2}$. For the ^{22}Na source data were acquired with an attenuator setting of 2 only. The channels corresponding to the Compton edges (defined as the point on the high energy side of the edge where the count rate had dropped by a factor of 2 from the peak) were determined from the γ-ray spectra and plotted in figure II.E-1. The data acquired with the $\sqrt{2}$ attenuator setting were normalized to a setting of 2 by multiplying the γ-ray energy by a factor of $\sqrt{2}$ then plotting.

F. Electronics

To measure the β-γ circular polarization correlation asymmetry, an electronics set up that records events producing logic signals in all three detectors (a three-fold coincidence) is required. With η approximately equal to 0.03 the expected measured value of $(N_+ - N_-)/(N_+ + N_-)$ is about 0.004 for the $^{24}Al(\beta^+)^{24}Mg^*(8.437\ MeV)(\gamma)^{24}Mg^*(1.369\ MeV)$ decay sequence. The statistical error of $(N_+ - N_-)/(N_+ + N_-)$ is about $1/\sqrt{(N_+ + N_-)}$ for such a small asymmetry. Therefore, to obtain a statistical error of about 0.001, one must have $(N_+ + N_-)$ equal about 10^6. Combining these estimates with the attenuation of the γ rays passing through the polarimeter, the branching ratio of the $^{24}Al(\beta^+)^{24}Mg^*(8.437\ MeV)$ decay and the NaI γ ray efficiency, it is found that the singles rates in the plastic and the surface barrier detectors must be about 1 MHz to obtain a statistical error of about 0.001 in approximately ten days of

Figure II.E-1 Calibration curve for plastic detector. All points were normalized to an attenuation factor of 2 before plotting.

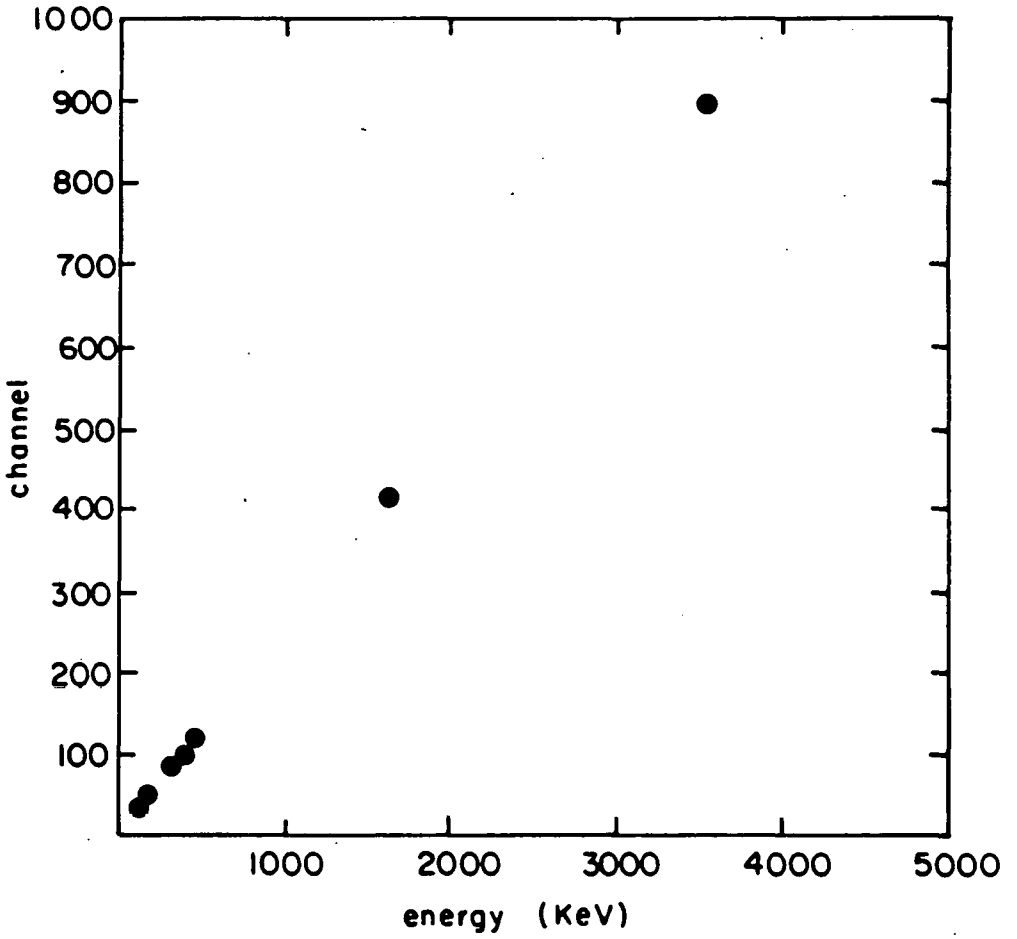
1000
900
800
700
600
500
400
300
200
100
channel
1000
2000
3000
4000
5000
energy (KeV)

running time. Therefore, the fast negative signals from the plastic and surface barrier detectors were used as linear signals as well as timing signals.

The fast signals from the plastic and surface barrier detectors are respectively 20 ns and 40 ns long. With these fast signals there is no significant pile up for singles rates of 2-3 MHz. The electronics scheme used to acquire data primarily used fast LeCroy electronics for generating logic signals and digitizing of fast signals (a detailed electronics diagram is given in figure II.F-1). The fast signals from the plastic and surface barrier detectors were fanned out; one of the fanned out signals from each detector was used to generate a coincidence output from a LeCroy model 465 overlap coincidence unit (this will be called a 2-fold coincidence). The input signals to the LeCroy 465 were generated by feeding the fanned out signals into Berkeley constant fraction discriminators (CFD's). The CFD outputs were then used to fire LeCroy model 821 discriminators which have adjustable output pulse widths. The 821 outputs were then fed to the 465 coincidence unit. The timing of the input of the signals to the coincidence unit is shown in figure II.F-2. Since the plastic signal had less time jitter than the surface barrier signal, its input to the coincidence unit was made shorter than the surface barrier input and hence determined the time of the coincidence output. The remaining fanned out signals from the plastic and surface barrier detectors were used as linear signals. These signals were digitized in a LeCroy 2249A charge sensitive ADC which integrates the charge in a fast negative signal.

Figure II.F-1 Diagram of electronics used to collect 3-fold coincidence data.

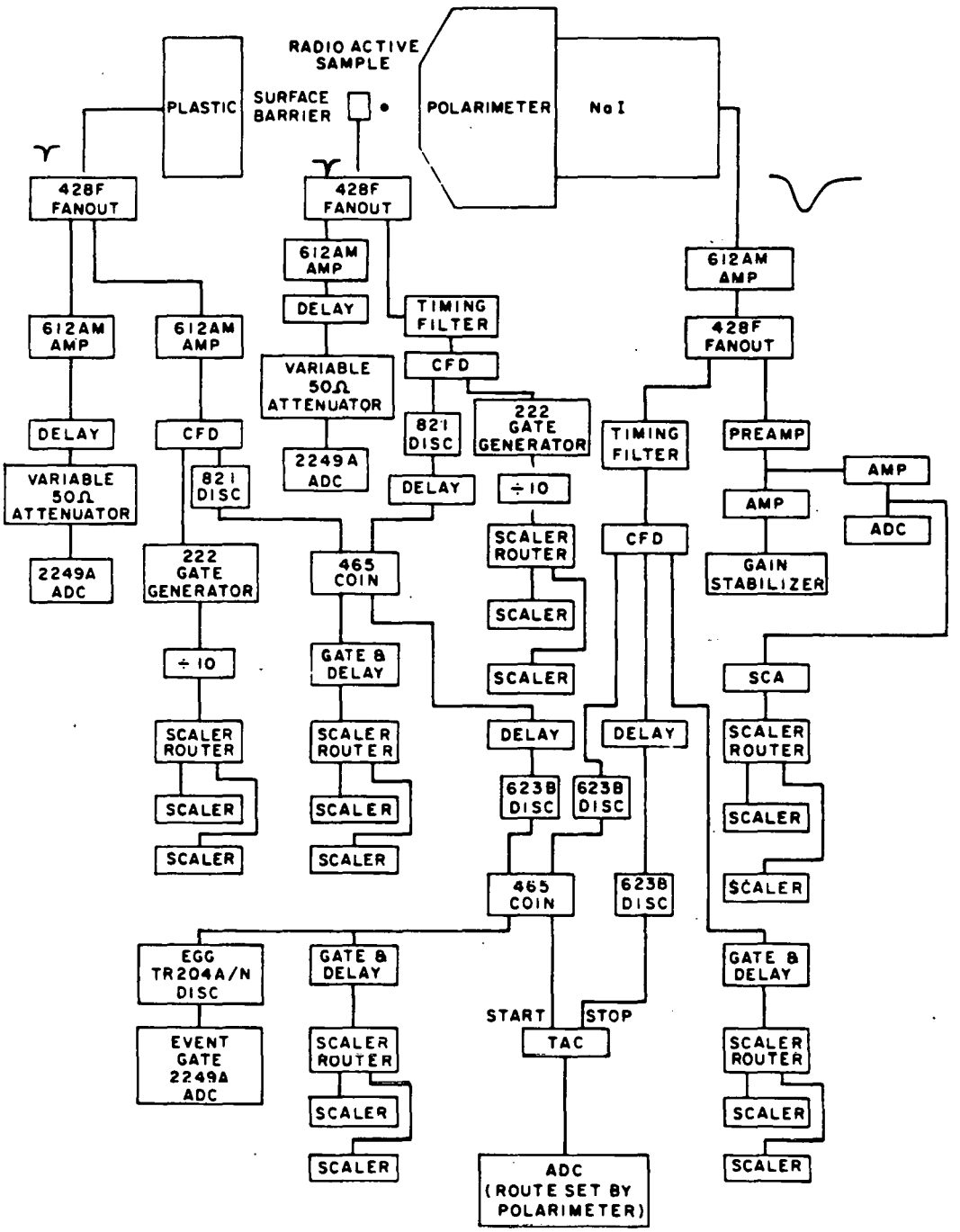
RADIO ACTIVE SAMPLE
PLASTIC
SURFACE BARRIER
POLARIMETER
NoI
γ
γ
428F FANOUT
428F FANOUT
612AM AMP
612AM AMP
612AM AMP
DELAY
TIMING FILTER
612AM AMP
428F FANOUT
VARIABLE 50Ω ATTENUATOR
CFD
DELAY
CFD
821 DISC
222 GATE GENERATOR
TIMING FILTER
PREAMP
AMP
VARIABLE 50Ω ATTENUATOR
821 DISC
2249A ADC
DELAY
÷10
CFD
AMP
ADC
2249A ADC
222 GATE GENERATOR
465 COIN
SCALER ROUTER
GAIN STABILIZER
SCALER
÷10
GATE & DELAY
SCALER
SCA
SCALER ROUTER
SCALER ROUTER
DELAY
DELAY
SCALER ROUTER
SCALER
SCALER
6238 DISC
6238 DISC
SCALER
SCALER
SCALER
465 COIN
6238 DISC
SCALER
EGG TR204A/N DISC
GATE & DELAY
GATE & DELAY
START
STOP
EVENT GATE 2249A ADC
SCALER ROUTER
TAC
SCALER ROUTER
SCALER
SCALER
SCALER
ADC (ROUTE SET BY POLARIMETER)
SCALER

Due to attenuation in the polarimeter the singles rate in the NaI was limited to approximately 35 kHz. With this rate and anode signals approximately 500 ns long pile up was no problem with standard slow electronic processing. The NaI anode signal was used to generate a timing signal using a Berkeley CFD and a linear signal in the usual way. The NaI timing signal and the 2-fold coincidence output were fed to LeCroy model 623B discriminators with adjustable length outputs. The discriminator outputs were then fed to another 465 coincidence unit. The timing of these two coincidence inputs is shown in figure II.F-2. The NaI input to the coincidence unit was much longer than the 2-fold input so that the time of the plastic signal, via the 2-fold coincidence, determined the time of this coincidence output (this will be called a 3-fold coincidence). The 3-fold coincidence output gated the computer so that an event was required to produce a signal in all three detectors before it was considered a valid event by the computer.

In addition to providing a computer gate, the 3-fold coincidence output was used to start a Time to Amplitude Converter (TAC). The stop for the TAC was derived from the NaI signal with an appropriate delay. Singles rates in the plastic and surface barrier detectors were so high that stopping the TAC on either of these signals or the 2-fold coincidence would have rendered the TAC useless since the TAC would miss a large fraction of the good events due to dead time. The TAC signal recorded the time between the 3-fold signal and the NaI signal. The TAC signal was routed according to the state of the polarimeter and digitized in a standard Tracor Northern ADC.

Figure II.F-2 Timing diagram for 2-fold and 3-fold coincidences.

2 — fold coincidence timing

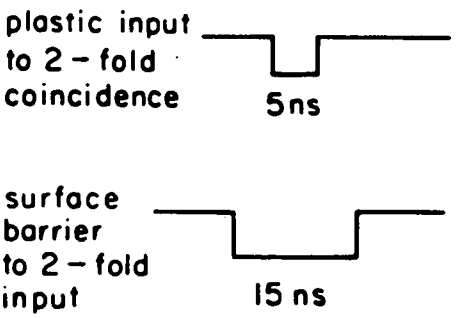

3 — fold coincidence timing

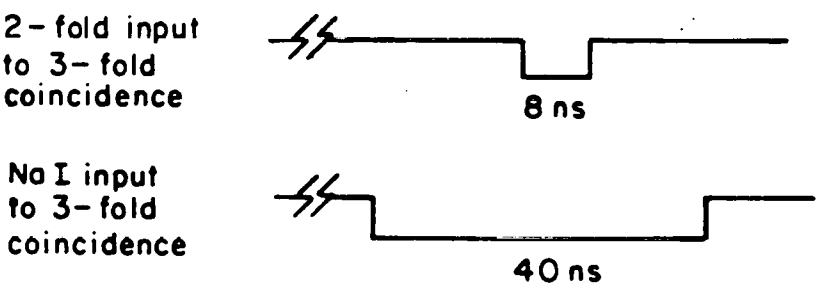

Along with the NaI and TAC signals, the output of the polarimeter sense coil was digitized in a standard Tracor Northern ADC. The output of the sense coil was fed to the level shifter. The output of the level shifter was set so that it was always between +0 and +10 volts for all magnet currents. This level was converted by the ADC and measured the magnetic field for each event.

In order to make dead time corrections and proper normalization of the data as well as to check for systematic asymmetries, the plastic, surface barrier and NaI singles, the 2-fold and 3-fold coincidences and a single channel analyzer (SCA) output were fed to routed scalers. The SCA had its window on the γ ray of primary interest. The TAC and all scaler routes were synchronized with the state of the polarimeter. The synchronization was controlled by the polarized ion source flipper box (Ad 73). The flipper box was operated in the external mode. The external input was a TTL output from the rabbit timer. The TTL signal was timed so that it turned on 0.5 seconds after the target left the counting station. When the polarized ion source flipper box received the rabbit signal it changed the state of two routing outputs simultaneously. One routing output set the 512 bit on the TAC spectrum. If the routing bit was off the TAC signal was between 0 and 511 and the odd numbered scalers counted; if the routing bit was on the TAC signal was between 512 and 1023 and the even numbered scalers counted.

The other routing bit set the state of the polarimeter flipping bridge. With the routing bit on the bridge always supplied positive current to the polarimeter from its positive terminal. When the

routing bit changed to off, the bridge flipped to supplying negative current from its positive terminal. The actual direction of the magnetic field in the polarimeter depended on how the outputs of the flipping bridge where connected to the inputs of the polarimeter coil. These connections were reversed periodically during every measurement so that any possible electronic bias that might be introduced by one route compared to the other was averaged out.

When the polarized ion source flipper box is given a start signal by the experimenter the box waits until a trigger is received from the rabbit timer and all routing bits are off before any data is acquired. When the experimenter gives the polarized ion source flipper box a stop signal, data is acquired until a counting period with all routing bits on is completed, then the experiment is stopped. For a steady beam producing the radioactive sample, this arrangement equalizes the number of decays for each route.

While the polarized ion source flipper box insures that all bits are correctly set, a LED-photo transistor interlock on the rabbit tube insures that no data will be acquired if the rabbit is not in the correct counting position. When the target is not in the counting position a LED on the rabbit tube shines on and biases a photo transistor on the other side of the rabbit tube. The output of this transistor controls a circuit that gates off the computer when the rabbit is not in the counting position. When the rabbit is in the counting position the LED light is blocked and the computer is not gated off by the photo transistor circuit.

Once an event has satisfied all the coincidence requirements, all

routing bits are set and the target is in the proper position the recording of signals in the fast and slow ADC's has to be synchronized. The slow NaI and TAC signals were approximately 2 μsec later in arriving at the ADC's than were the fast plastic and surface barrier signals. A time interlock control was built to synchronize the fast-signal and slow-signal data acquisition.

The 3-fold coincidence signal gated the fast LeCroy ADC and initiated the conversion of the fast signals. At this time the LeCroy ADC issued a busy signal which the time interlock control sensed. The time interlock control unit then generated an event-occur for the Tracor Northern ADC's. This event occur signal has an adjustable delay and width. With these adjustments the event-occur can be timed so that the late arriving slow signals are centered on the event-occur and a proper set of coincidence signals are recorded.

For every valid set of coincidence signals generated, the digitized plastic, surface barrier, and NaI detector signals, TAC and magnetic field signals were written on tape. The routing bits were recorded by the half of the spectrum the TAC signal was in and the polarity of the current input to the polarimeter was determined from the routing bits and the magnetic field signal.

CHAPTER III

EXPERIMENTAL RESULTS

A. Introduction

With any newly developed experimental apparatus measurements of well known quantities provide a necessary check on the performance of the apparatus. Three simple beta decays were studied to check the performance of the β-γ circular polarization correlation apparatus before the complex ^{24}Al beta decay was studied.

B. The β^- Decay of ^{28}Al

The β^- decay of ^{28}Al provided a convenient calibration of the β-γ circular polarization correlation apparatus where a large A is expected. The ^{28}Al was produced via the ^{27}Al(d,p)^{28}Al reaction using a 25 micron ^{27}Al foil target and a 6 MeV deuteron beam. The half life of ^{28}Al is 2.24 minutes. With this half life a rabbit cycle of 10 seconds (4.5 seconds in the beam, 4.5 seconds counting and 0.5 seconds for each transit) minimized the effects of short term beam fluctuations on the activity of the target. The ^{28}Al β^- decay (beta end point energy = 2.864 MeV) goes 100% of the time to the first excited state in ^{28}Si, which γ decays, emitting a 1.778 MeV γ ray, to the ground state. The spin sequence for this decay is $3^+ \rightarrow 2^+ \rightarrow 0^+$. This spin sequence implies a pure Gamow-Teller beta decay ($\Delta J = 1$), pure E2 γ radiation and, using equation I.F-5, a large A (= -1/3).

Typical spectra for the NaI, TAC, surface barrier and plastic signals are shown in figures III.B-1 to III.B-4. The ΔE signal from the surface barrier detector was scaled so that it had the same energy calibration as the plastic E signal. The E and ΔE signal were then added together to get the total β energy signal. The total energy signal along with the calculated expected β energy distribution is shown in figure III.B-5. The finite resolution of the detectors and the scattering of some of the betas tends to distort the shape of the measured distribution. However, the overall agreement with the expected shape is reasonably good.

The quantities N_+ and N_- were calculated from events with γ-ray energies in the upper 15% of the NaI spectrum. A routed TAC spectrum was generated from all events in the upper 15% of the NaI spectrum. Three equal size windows were placed on each route of the TAC spectrum. One window was on the TAC peak, and one window was on the random background on each side of the TAC peak. The number of real coincidences for each route was then calculated by forming the quantity (sum of events in the peak window) - (sum of events in both random background windows)/2.

These peak areas were normalized to the same number of decays and dead-time corrected. The normalization was done with the SCA scalers. The SCA had its window on the photo peak of the 1.778 MeV γ ray. To correct for any difference in the number of decays and any small gain shift in the NaI detector for the two routes N_+ was multiplied by $(N_{SCA-})/(N_{SCA+})$ where $N_{SCA+(-)}$ is the SCA scaler count for the +(-) route. The dead-time correction was done using the TAC route sums and

Figure III.B-1 NaI spectrum for the ^{28}Al β^- decay showing the single 1.778 MeV γ ray.

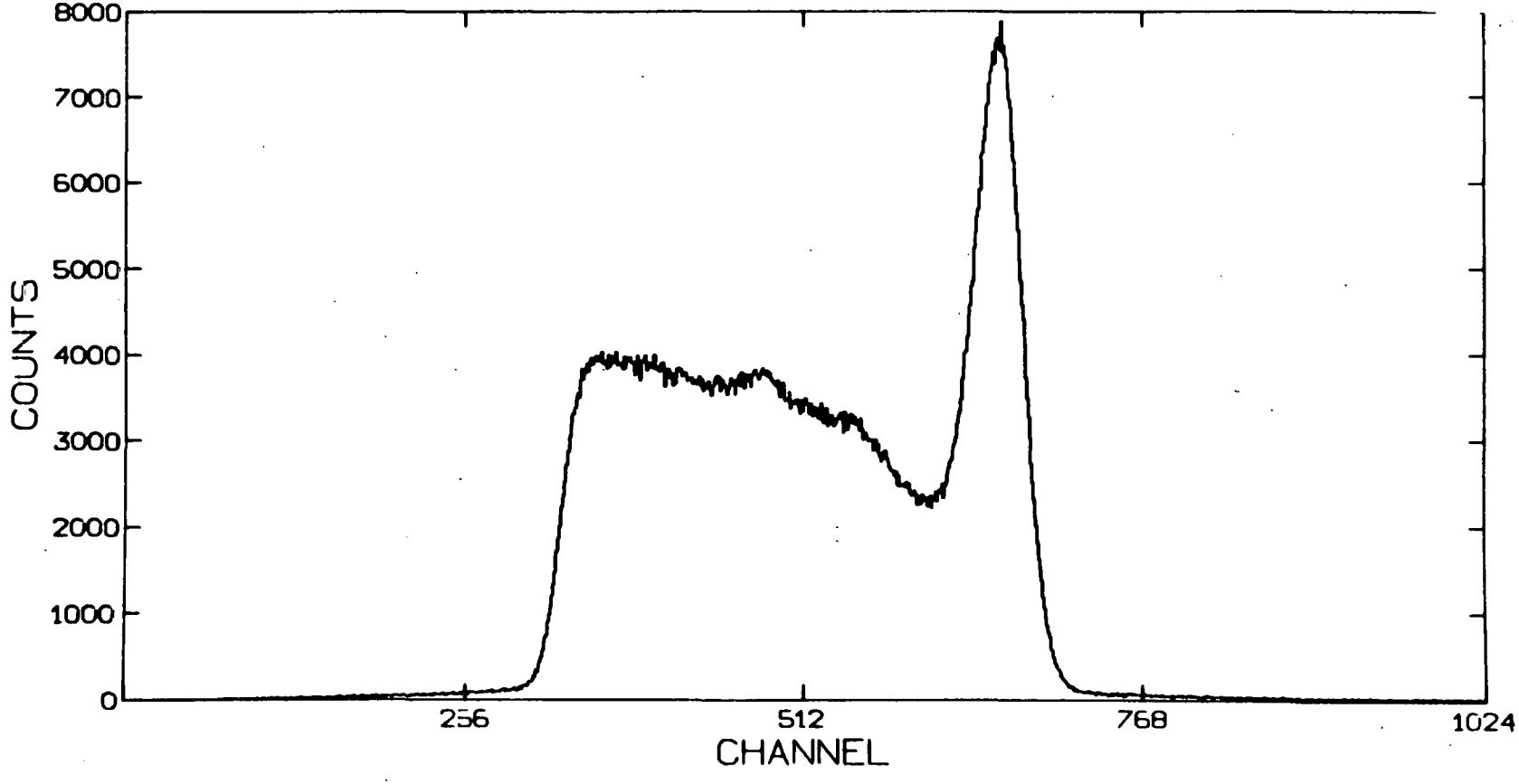
8000
7000
6000
5000
4000
3000
2000
1000
0
COUNTS
256
512
768
1024
CHANNEL

Figure III.B-2 TAC spectrum for the ^{28}Al β^- decay. One channel equals 0.17 ns.

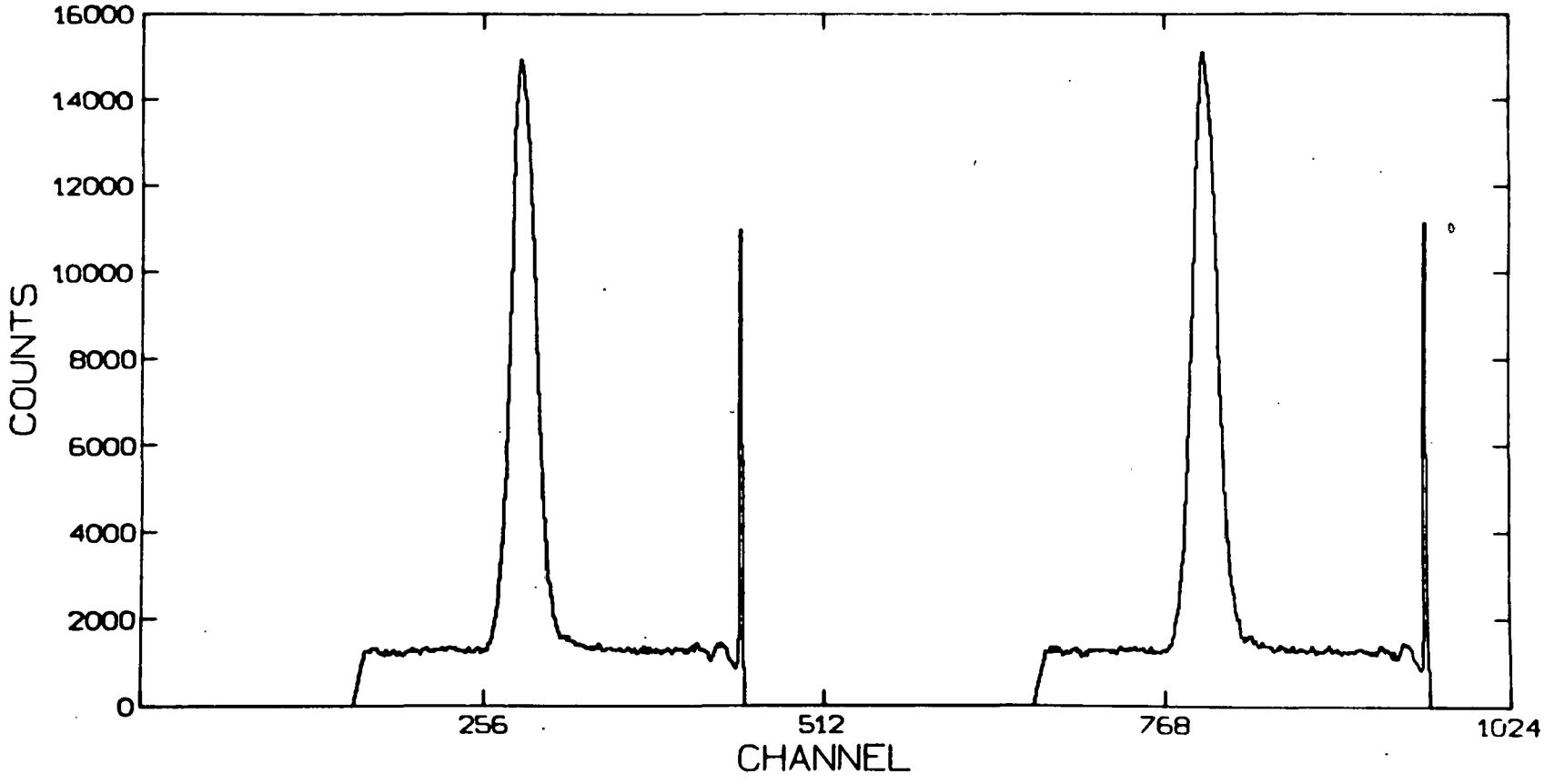
16000
14000
12000
10000
8000
6000
4000
2000
0
COUNTS
256
512
768
1024
CHANNEL

Figure III.B-3 Surface barrier detector spectrum for the ^{28}Al β^- decay.

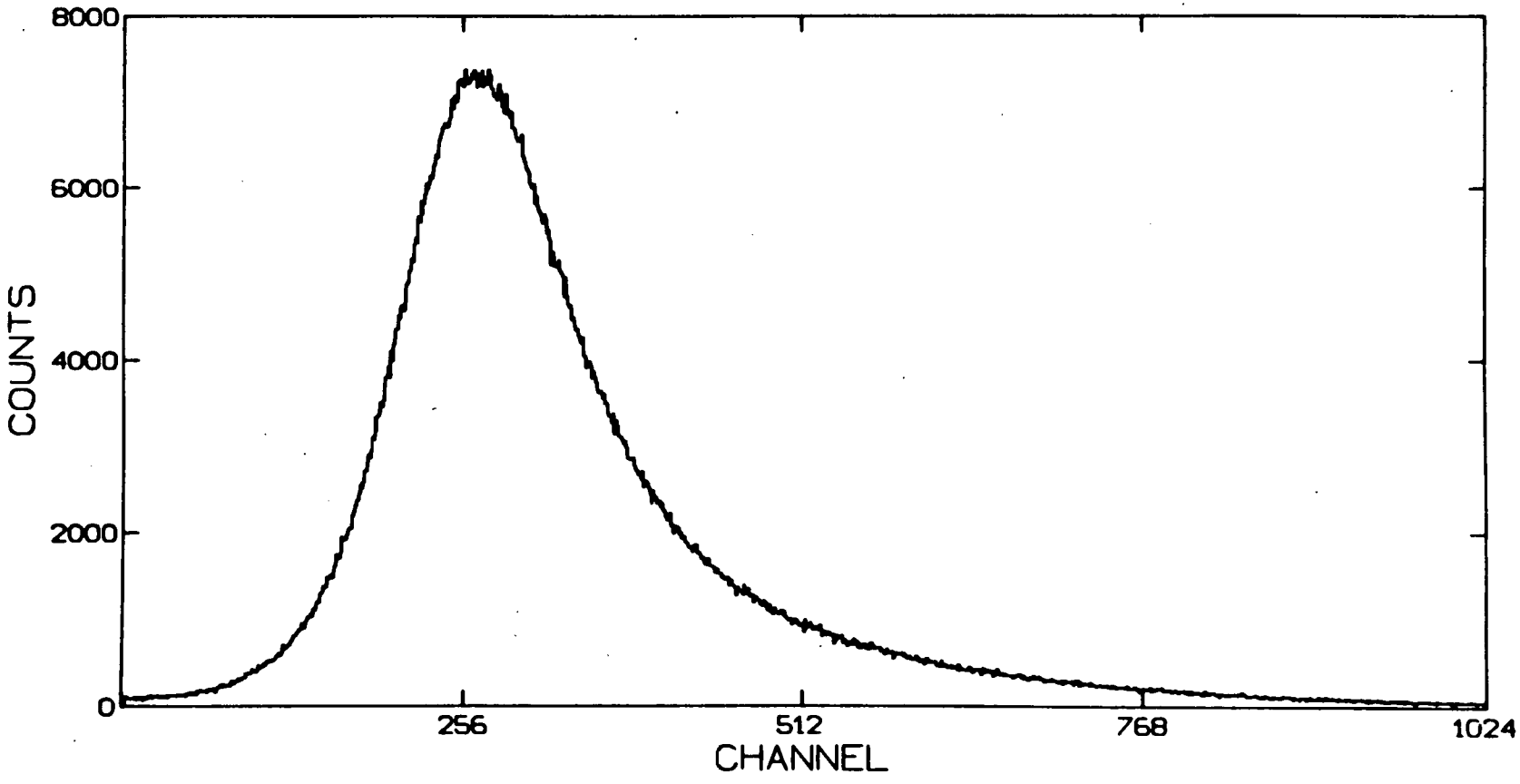
8000
6000
4000
2000
0
COUNTS
256
512
768
1024
CHANNEL

Figure III.B-4 Plastic detector spectrum for the ^{28}Al β^- decay.

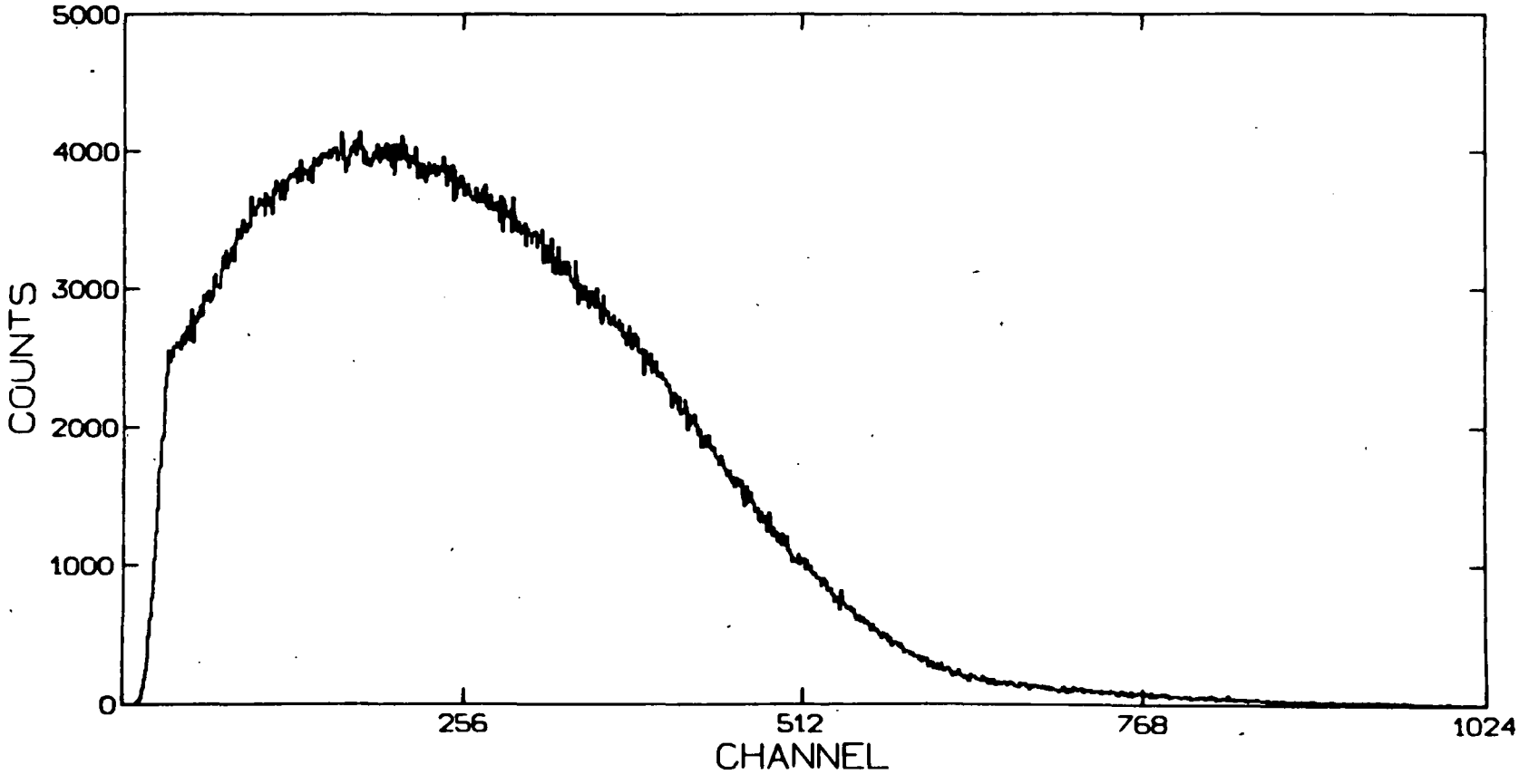
5000
4000
3000
2000
1000
0
COUNTS
256
512
768
1024
CHANNEL

Figure III.B-5 Total β^- energy spectrum for the ^{28}Al decay. The surface barrier detector signal has its gain adjusted so that it has the same energy calibration as the plastic detector. The two signals are then added to form this spectrum. The solid curve represents the calculated allowed shape for this decay.

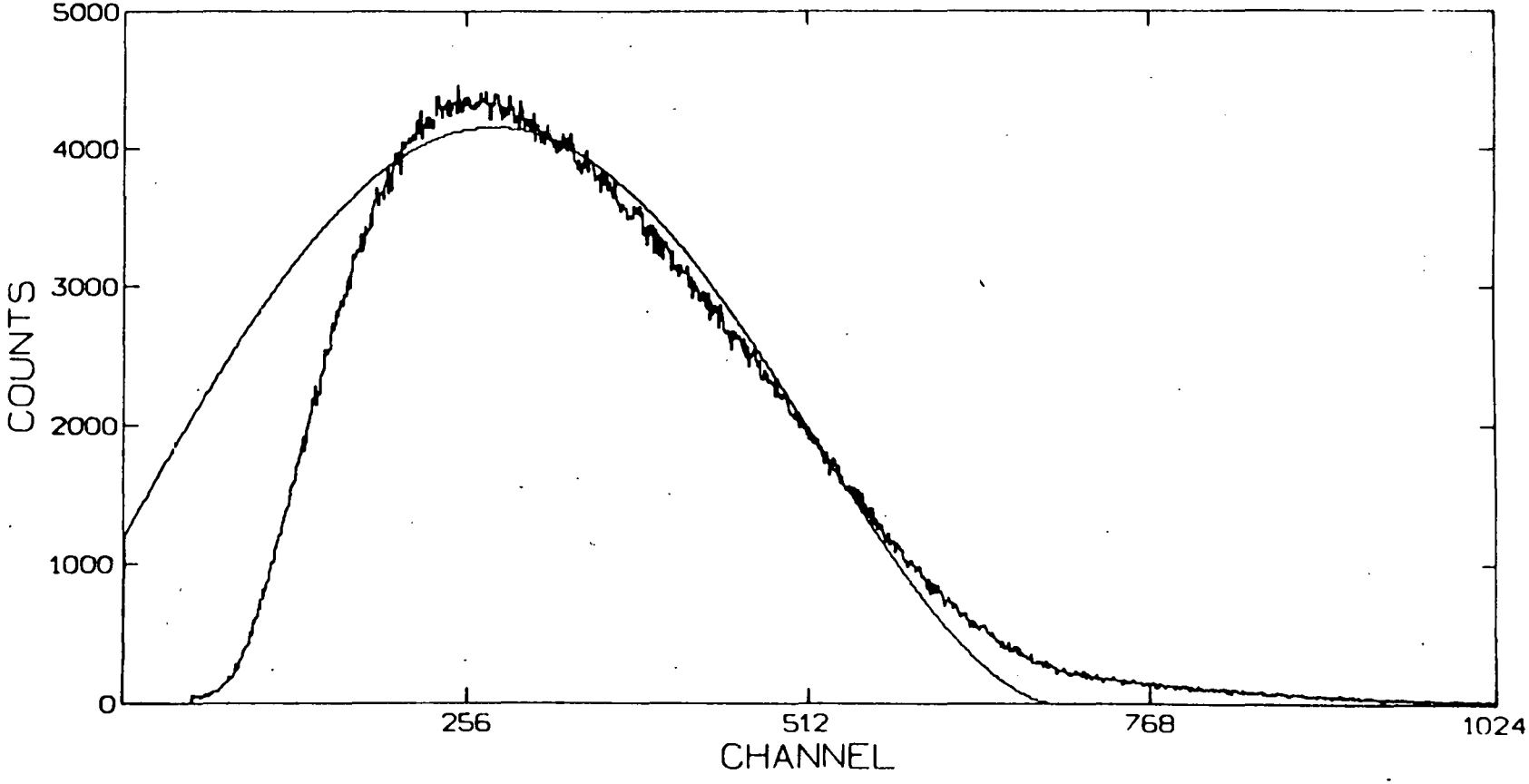
5000
4000
3000
2000
1000
0
COUNTS
256
512
768
1024
CHANNEL

the routed 3-fold coincidence scalers. N_+ was corrected for relative dead time by the factor $(3\text{-fold}_+/\text{sum}_+)\times(\text{sum}_-/3\text{-fold}_-)$ where $3\text{-fold}_{+(-)}$ are the routed scaler totals and $\text{sum}_{+(-)}$ is the TAC route sum for the +(-) route. Using the corrected N_+ and N_- and

$$A = \frac{N_+ - N_-}{N_+ + N_-} \frac{1}{\eta \langle v/c \rangle \langle \cos(\theta) \rangle}$$

where $\langle v/c \rangle$ = average value of v/c for the betas that pass through the surface barrier detector. This was calculated using the allowed beta shape and the stopping power of the surface barrier detector.

$= 0.948$

$\langle \cos(\theta) \rangle$ = value of $\cos(\theta)$ averaged over the solid angle of the detector system.

$= 0.938$

η = the polarimeter efficiency for a 1.778 MeV γ ray

$= 0.03090 \pm 0.00073$

The asymmetry A was calculated for 19 separate ^{28}Al runs. Combining all runs,

$$A = -0.318 \pm 0.025$$

which agrees quite well with the predicted value of -1/3. The χ^2 per degree of freedom for these runs was 0.60.

C. The β^+ Decay of ^{27}Si

The β^+ decay of ^{27}Si was used to check for any differences between the detection of positrons and of electrons. The ^{27}Si β^+

decay (beta end point energy = 3.787 MeV) goes to the ground state of ^{27}Al 99.8% of the time. Therefore, no circular polarization measurement was possible, but a comparision of β^+ and β^- spectra was made.

The ^{27}Si was produced via the $^{27}Al(p,n)^{27}Si$ reaction using a 7 MeV proton beam and a 25 micron ^{27}Al foil target. The half life of ^{27}Si is 4.14 seconds. The same 10 second rabbit cycle was used. The positrons were detected with the 3-fold coincidence unit but requiring only a 2-fold input signal (i.e. no γ signal was required).

The plastic and surface barrier signals are shown in figures III.C-1 and III.C-2 respectively. The only qualitative difference between the spectra for positrons and electrons is the presence of 511 keV γ rays in the positron plastic spectrum. The 511 keV γ rays are a result of the positron scattering. A positron emitted into the solid angle subtended by the telescope can generate a ΔE signal in the surface barrier detector, then scatter out of the surface barrier detector, miss the plastic, annihilate and emit a 511 keV γ ray that is detected by the plastic. Similarly, a positron not emitted into the solid angle of the telescope can scatter into the surface barrier detector, generate a ΔE signal, miss the plastic and annihilate, emitting a 511 keV γ ray into the plastic. These 511 keV γ rays result from real 2-fold coincident events, and therefore are expected in all β^+ spectra. The $E + \Delta E$ spectrum for the ^{27}Si decay is shown in figure III.C-3. For this spectrum only plastic signals above the Compton edge of the 511 keV γ rays were considered. The result is similar to the result for the ^{28}Al decays.

Figure III.C-1 Plastic spectrum for the ^{27}Si β^+ decay.

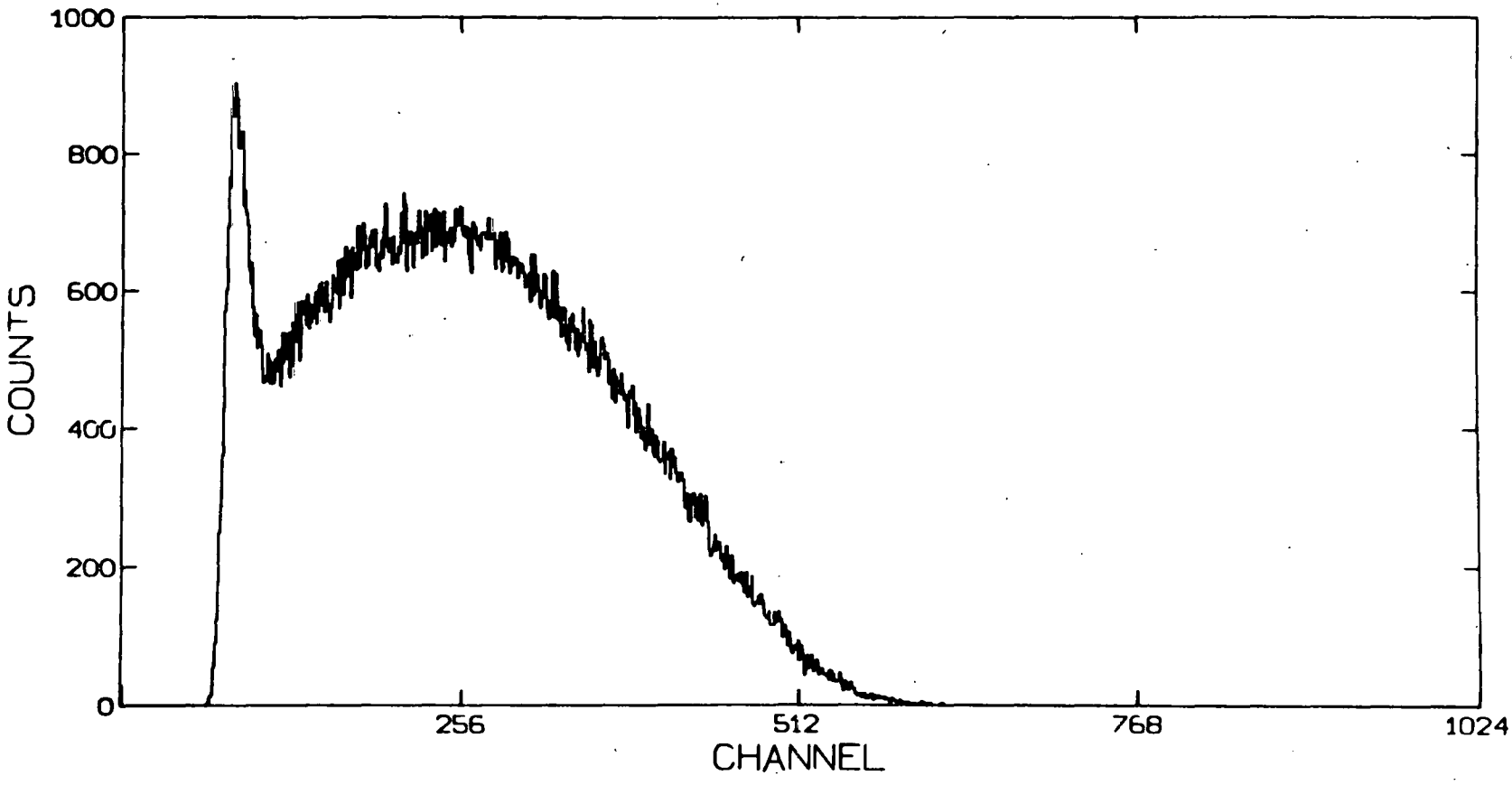
1000
800
600
400
200
0
COUNTS
256
512
768
1024
CHANNEL

Figure III.C-2 Surface barrier spectrum for the ^{27}Si β^+ decay.

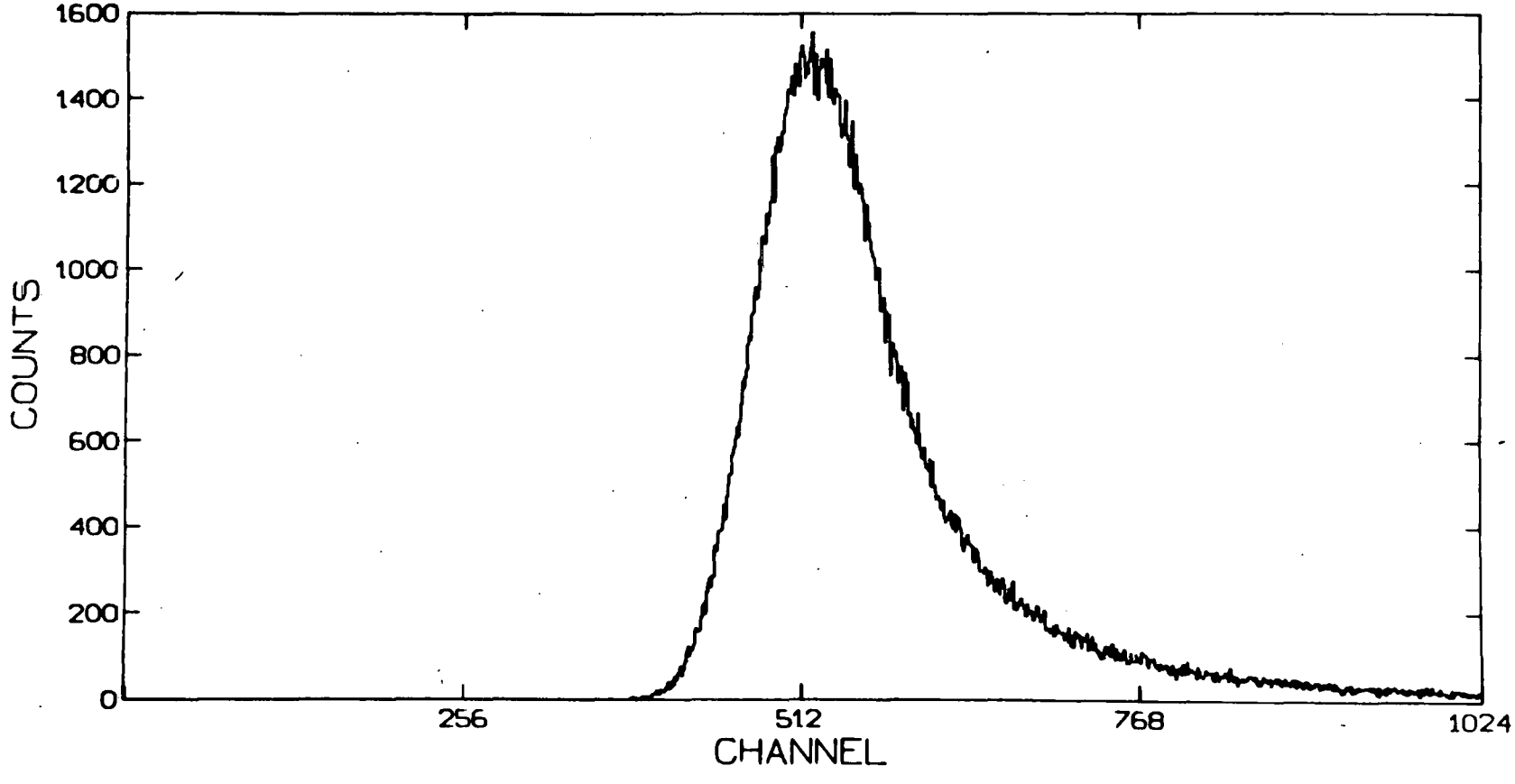
1600
1400
1200
1000
800
600
400
200
0
COUNTS
256
512
768
1024
CHANNEL

Figure III.C-3 Total β^+ energy spectrum for the ^{27}Si decay. The surface barrier detector has its gain adjusted so that it has the same energy calibration as the plastic detector. All the plastic signals above the Compton edge of the 511 keV γ ray are then added to the surface barrier signals to form this spectrum. The solid curve represents the calculated allowed shape for this decay.

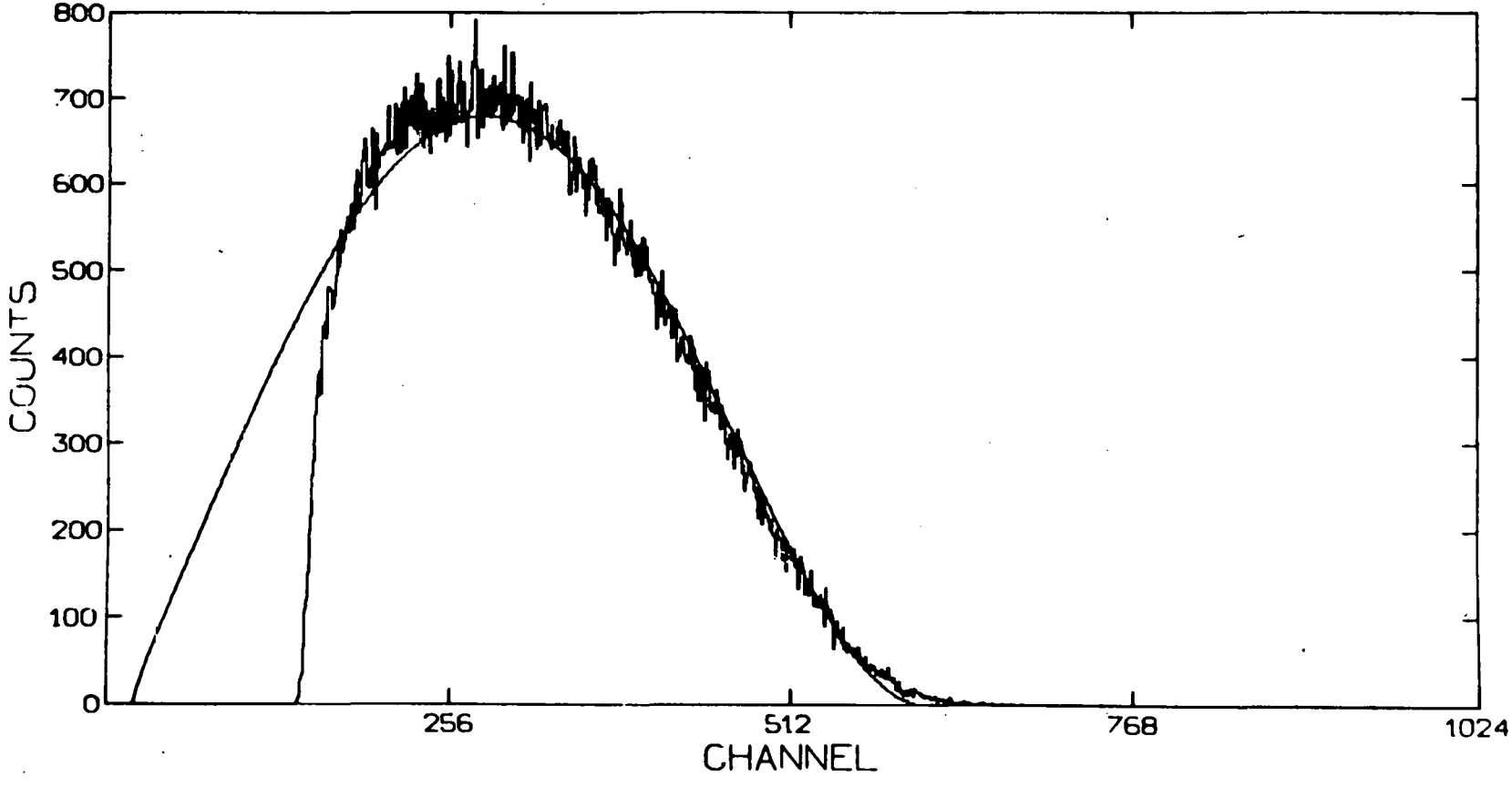
800
700
600
500
400
300
200
100
0
COUNTS
256
512
768
1024
CHANNEL

D. The β^+ Decay of ^{14}O

A zero calibration of the apparatus was done with the β^+ decay of ^{14}O. The ground state of ^{14}O is a 0^+, T=1 state that decays 99.4% of the time to the first excited state of ^{14}N which is a 0^+, T=1 state that emits a 2.313 MeV γ ray. The $0^+ \rightarrow 0^+$ nature of this decay insures that the circular polarization asymmetry must be 0.

The ^{14}O was produced via the $^{12}C(^3He,n)^{14}O$ reaction using a 10.5 MeV ^3He beam. The half life of ^{14}O is 70.5 seconds. The same 10 second rabbit cycle was used. Typical NaI, TAC, surface barrier and plastic spectra are shown in figures III.D-1 to III.D-4. The 1835 keV end-point energy of the ^{14}O decay is so low that most of the β^+ spectrum is below the 511 keV γ ray Compton edge. The SCA window was on the photopeak of the 2313 keV γ ray.

A TAC spectrum for γ rays with energies in the upper 15% of the NaI spectrum was used to calculate N_+ and N_- for each run. The same random background subtraction procedure used in the ^{28}Al analysis was used in this case. The same normalization and dead time corrections were made on N_+. This measurement yielded

$$(N_+ - N_-)/(N_+ + N_-) = 0.00175 \pm 0.00262$$

for eight runs with a χ^2 per degree of freedom of 0.70. This agrees well with the expected value of 0.

E. The β^+ Decay of ^{24}Al

After demonstrating the capabilities of the β-γ circular

Figure III.D-1 NaI spectrum for the ^{14}O β^+ decay showing the single 2.313 MeV γ ray.

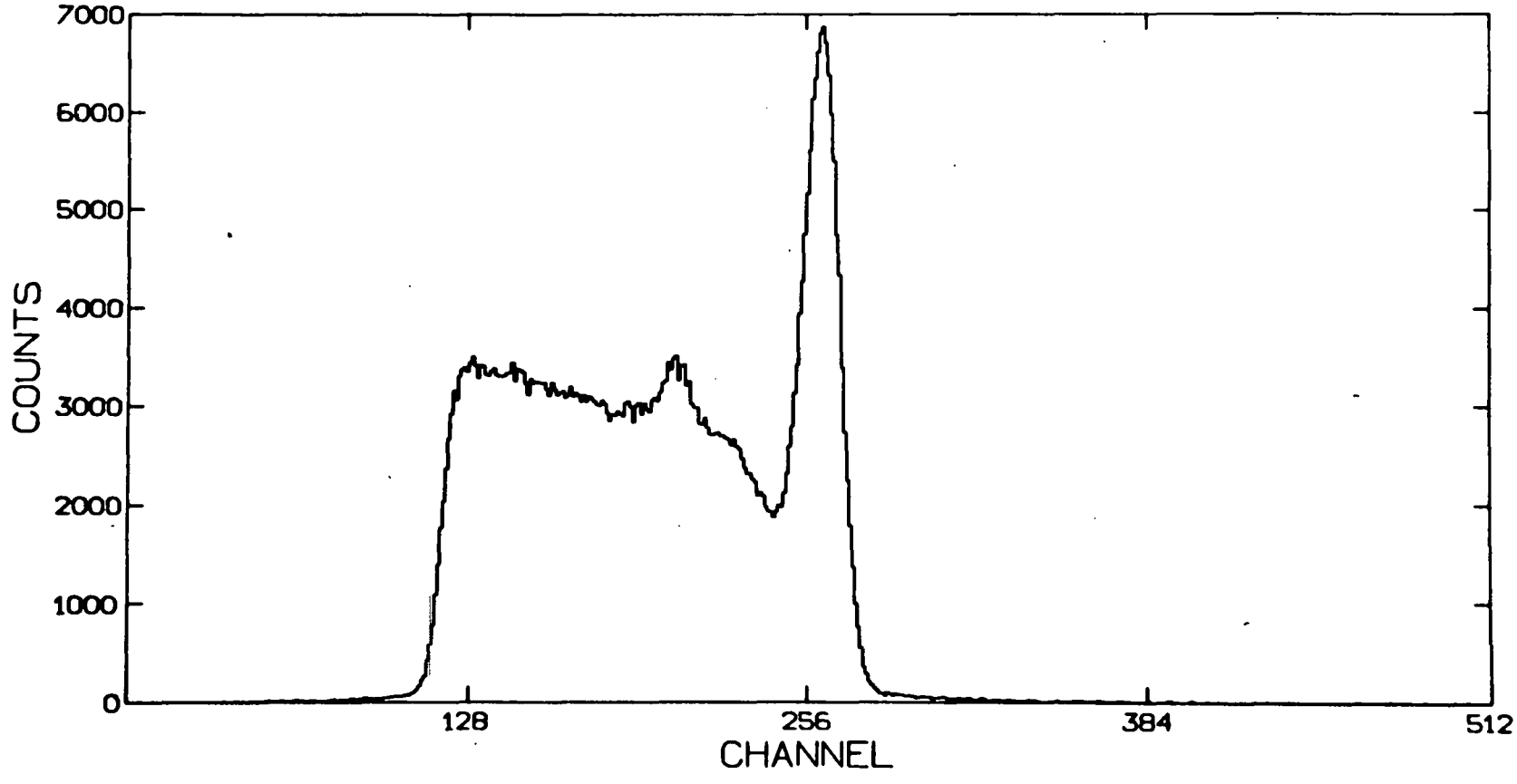
7000
6000
5000
4000
3000
2000
1000
0
COUNTS
128
256
384
512
CHANNEL

Figure III.D-2 TAC spectrum for the ^{14}O β^+ decay. One channel equal 0.17 ns.

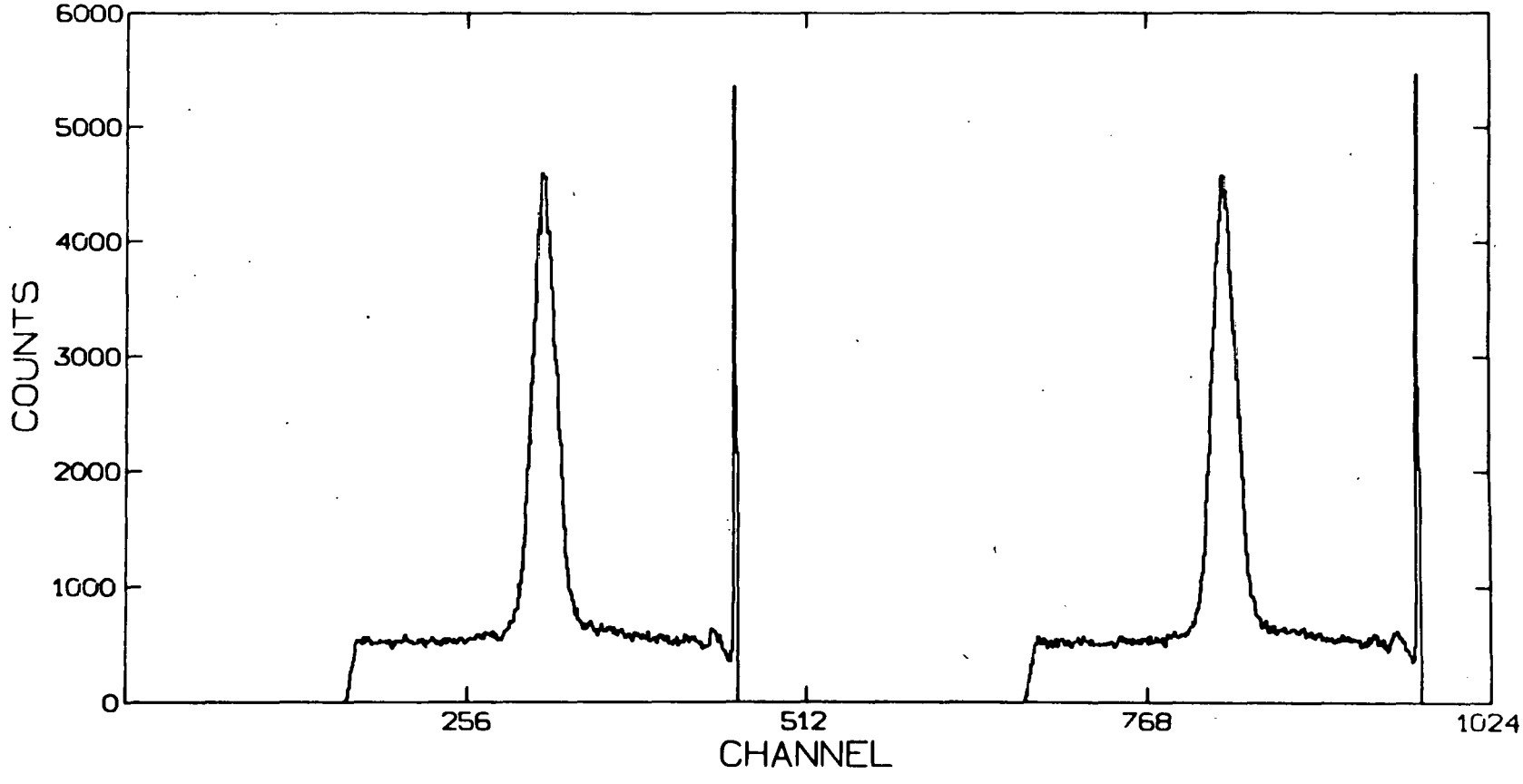
6000
5000
4000
3000
2000
1000
0
COUNTS
256
512
768
1024
CHANNEL

Figure III.D-3 Surface barrier detector spectrum for the ^{14}O β^+ decay.

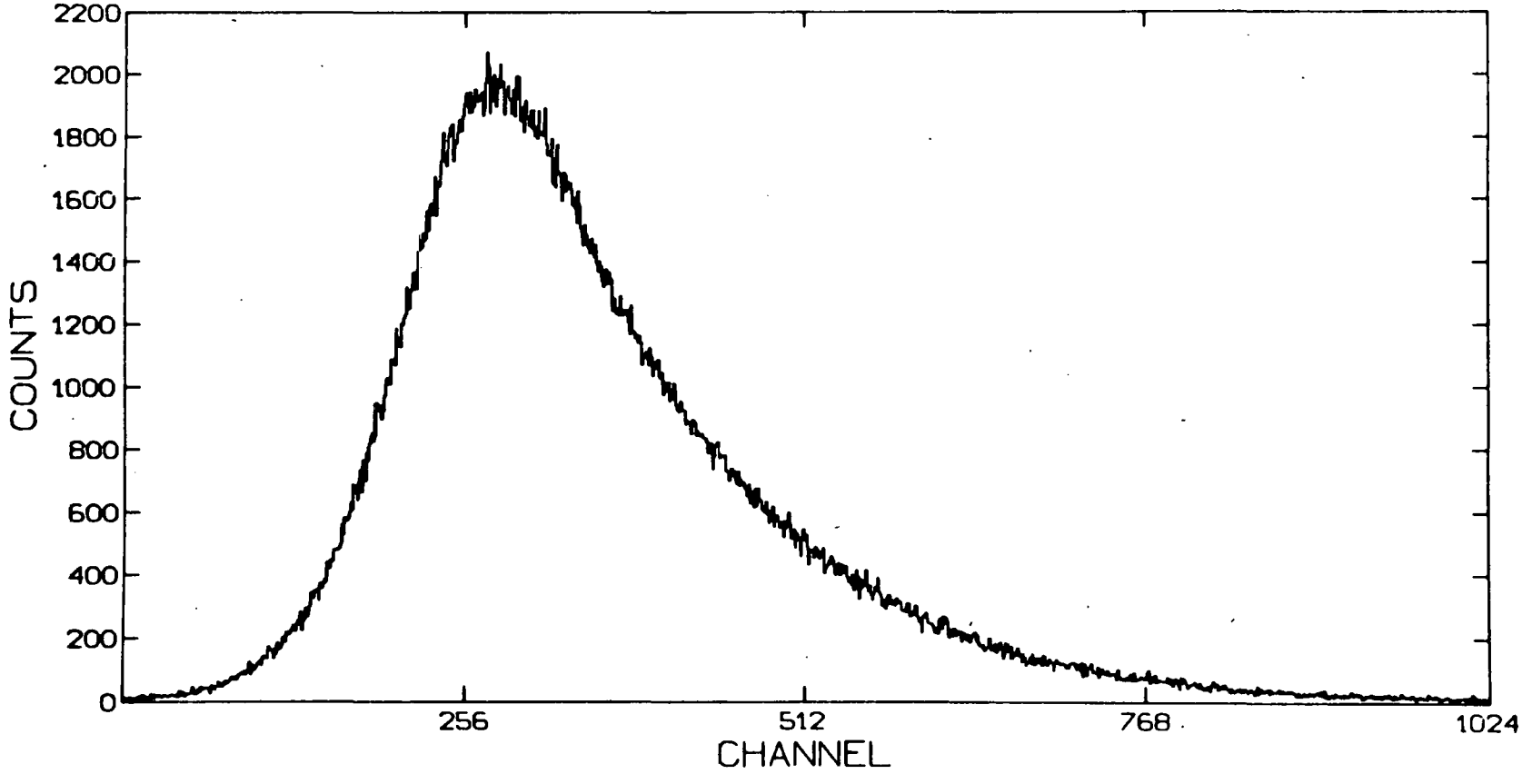
2200
2000
1800
1600
1400
1200
1000
800
600
400
200
0
COUNTS
256
512
768
1024
CHANNEL

Figure III.D-4 Plastic detector spectrum for the ^{14}O β^+ decay.

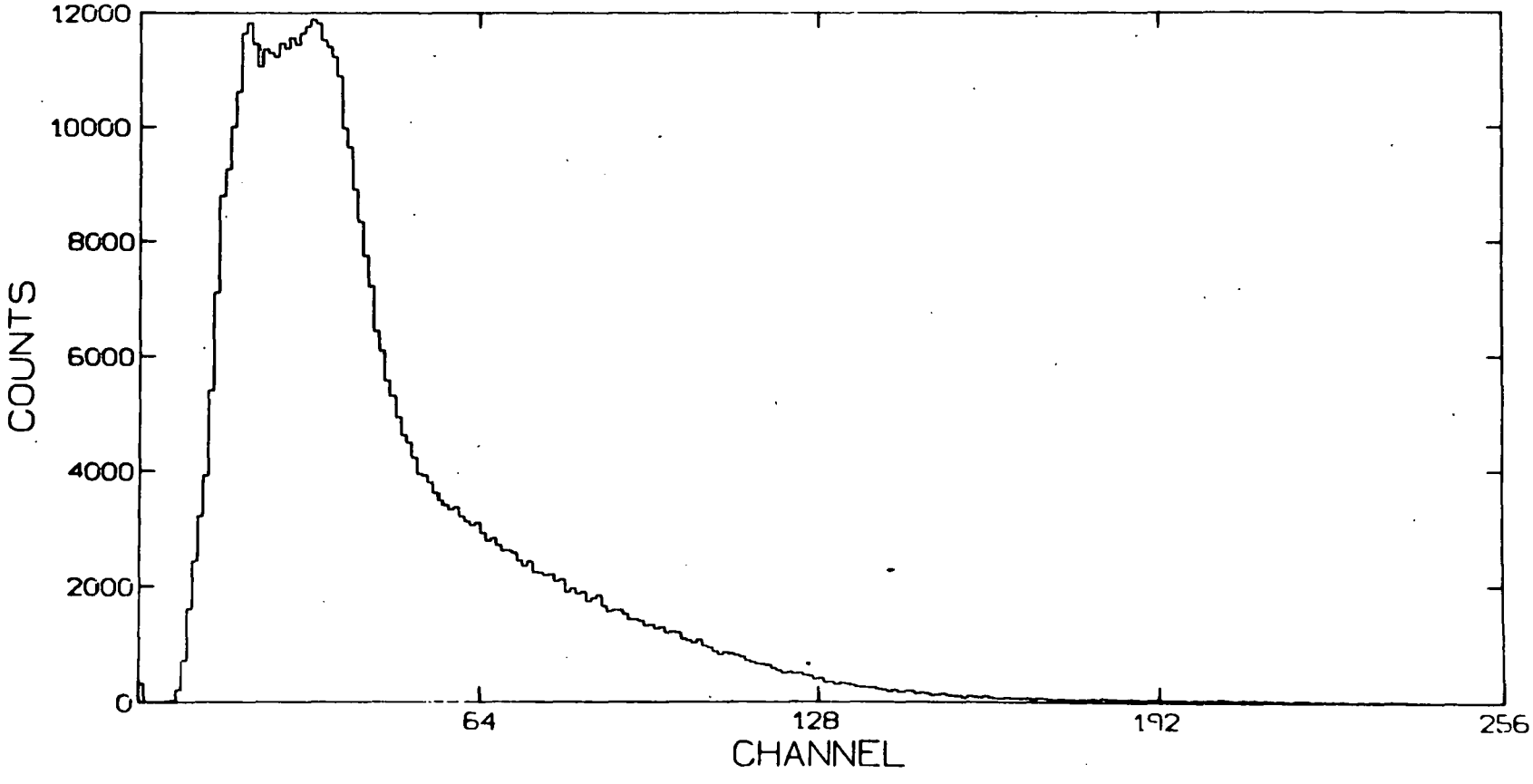
12000
10000
8000
6000
4000
2000
0
COUNTS
64
128
192
256
CHANNEL

polarization correlation apparatus, A was measured for two of the β^+ decay branches of ^{24}Al. The $^{24}Al(\beta^+)^{24}Mg^*(4.123\ MeV)(\gamma)^{24}Mg^*(1.369\ MeV)$ sequence (beta end point energy = 8.734 MeV) was previously done (Ha 63, Bl 64) and provided another performance check on the apparatus. The $^{24}Al(\beta^+)^{24}Mg^*(8.437\ MeV)(\gamma)^{24}Mg^*(1.369\ MeV)$ sequence (beta end point energy = 4.419 MeV) has not previously been done. The asymmetry in this sequence measures the isospin mixing between the 4^+, T=1 analog state at 9.515 MeV and the 4^+, T=0 state at 8.437 MeV where the mixing is expected to be the largest (see chapter 1).

The ^{24}Al was produced via the $^{24}Mg(p,n)^{24}Al$ reaction using an 18 MeV proton beam and a 180 micron natural magnesium target. The half life of the ground state of ^{24}Al is 2.07 seconds, and the half life of the ^{24}Al isomer at 440 keV is 0.129 seconds. A rabbit cycle of 7 seconds (3 seconds in the beam, 3 seconds counting and 0.5 seconds for each transit) was used. With the 0.5 second transit time most of the isomer decayed before the target reached the counting position (Ho 81).

Typical NaI, TAC, surface barrier and plastic spectra are shown in figures III.E-1 to III.E-4. The asymmetry A for the β^+ decay to the 4^+, T=0 state at 8.437 MeV and subsequent γ decay to the 2^+ state at 1.369 MeV was calculated from those events with a 7.068 MeV γ ray. The window on the γ ray spectrum included the photo and first-escape peaks for the 7.068 MeV γ ray. There was no significant background for this γ ray. A further criterion that all events have a plastic signal above the Compton edge of the 511 keV γ ray was imposed to

Figure III.E-1 NaI spectrum for the ^{24}Al β^+ decay . Peak 1 is the 1.369 MeV γ ray from the 1.369 MeV to ground state transition. Peak2(2′) is the photo(first escape) peak for the 2.754 MeV γ ray from the 4.123 MeV to 1.369 MeV transition. Peak 3(3′) is the photo(first escape) peak for the 4.314 MeV γ ray from the 8.437 MeV to 4.123 MeV transition. Peak 4(4′) is the photo(first escape) peak for the 5.392 MeV γ ray from the 9.515 MeV to 4.123 MeV transition. Peak 5(5′) is the photo(first escape) peak for the 7.068 MeV γ ray from the 8.437 MeV to 1.369 MeV transition.

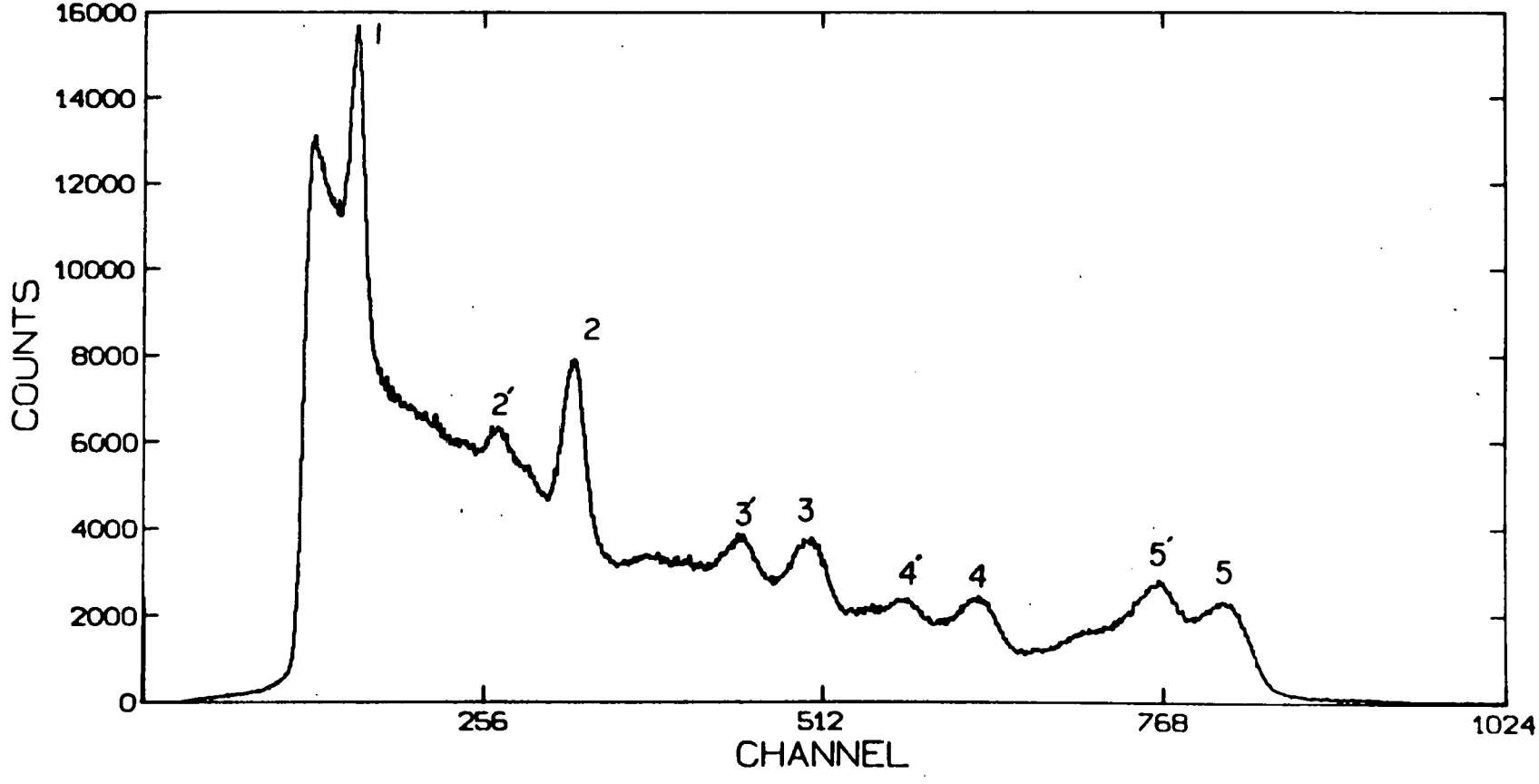
16000
14000
12000
10000
8000
6000
4000
2000
0
COUNTS
256
512
768
1024
CHANNEL
1
2´
2
3´
3
4´
4
5´
5

Figure III.E-2 TAC spectrum for the ^{24}Al β^+ decay. One channel equal 0.17 ns.

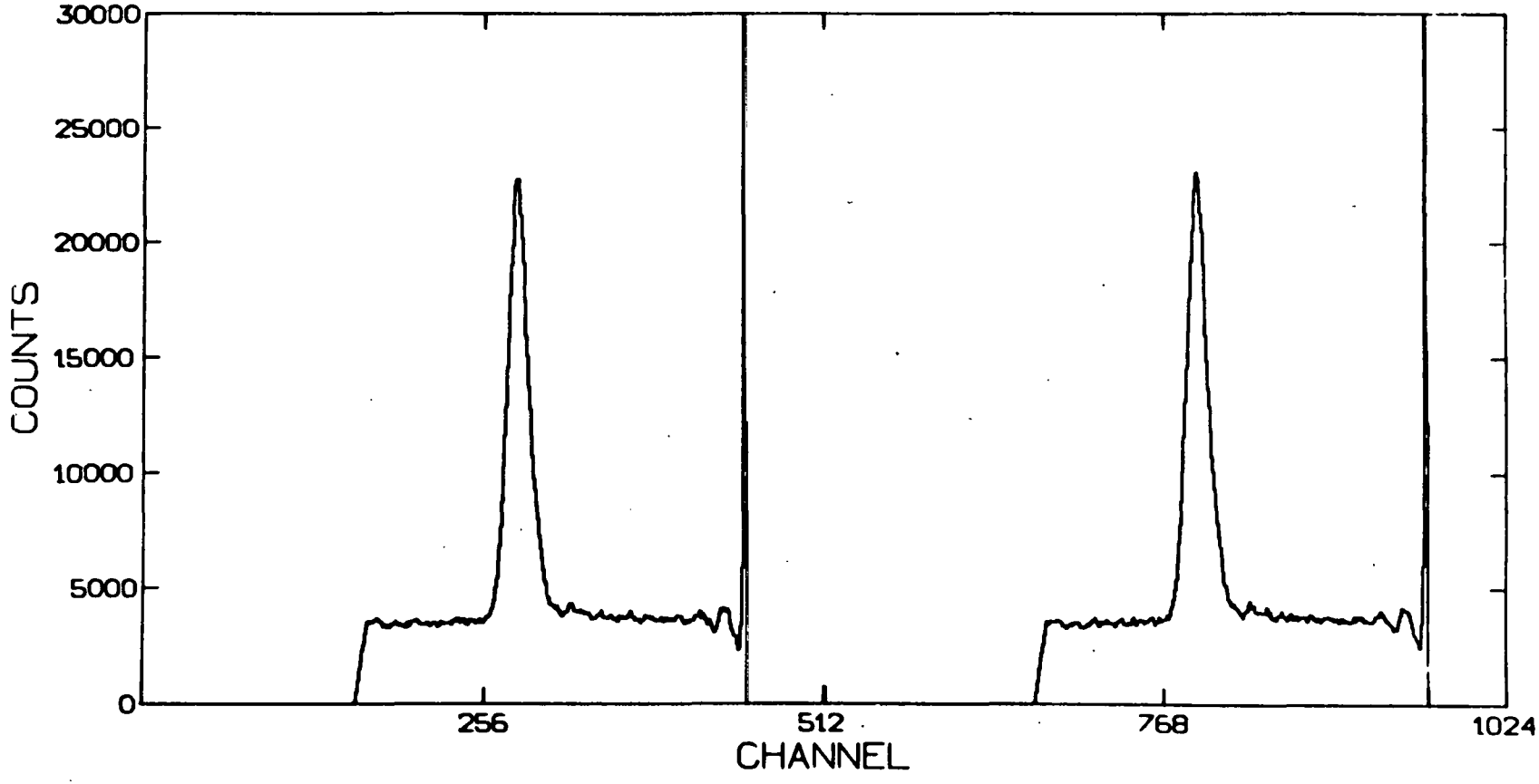
30000
25000
20000
15000
10000
5000
0
COUNTS
256
512
768
1024
CHANNEL

Figure III.E-3 Surface barrier detector spectrum for the ^{24}Al β^+ decay.

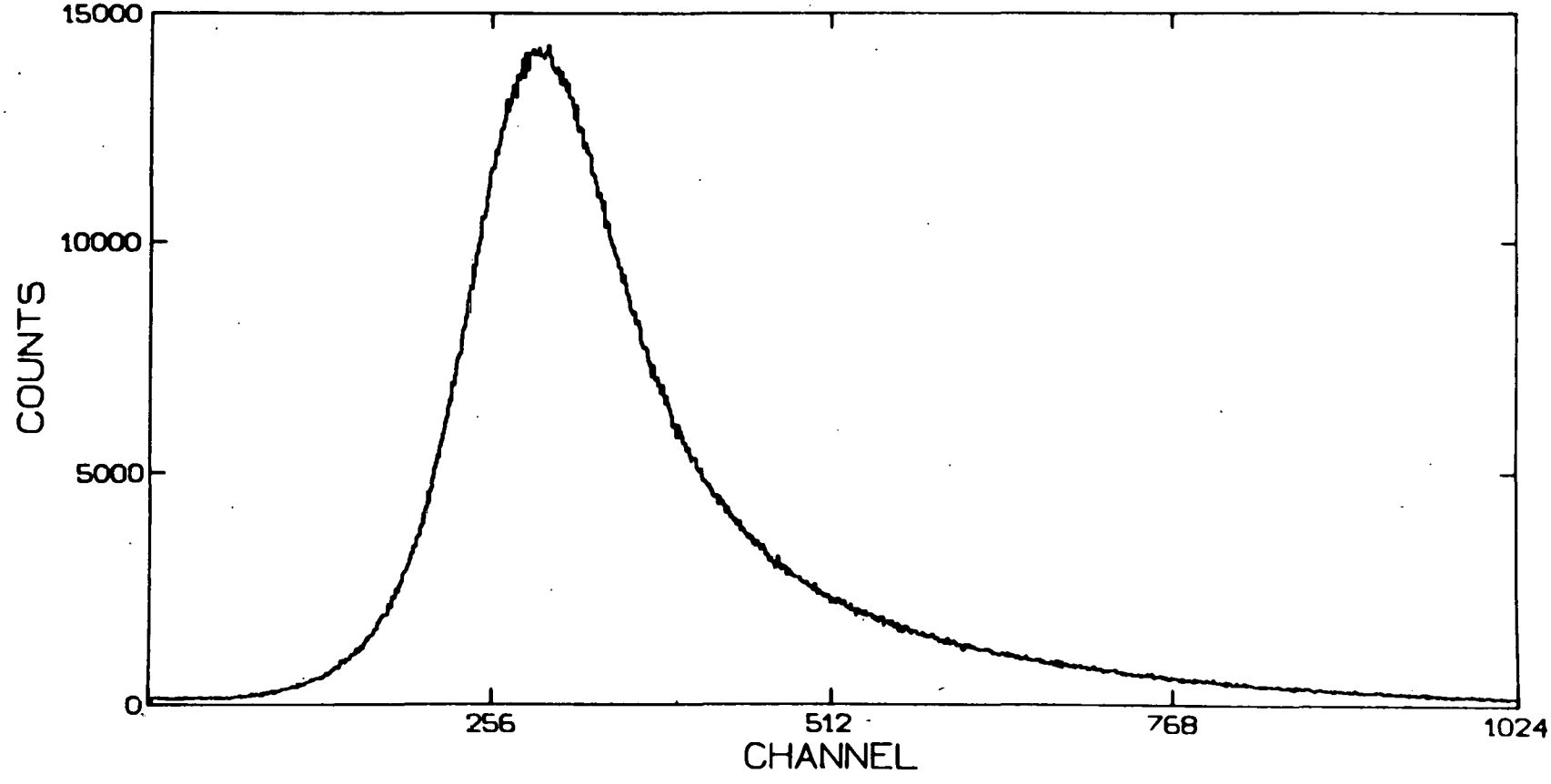
15000
10000
5000
0
COUNTS
256
512
768
1024
CHANNEL

Figure III.E-4 Plastic detector spectrum for the ^{24}Al β^+ decay.

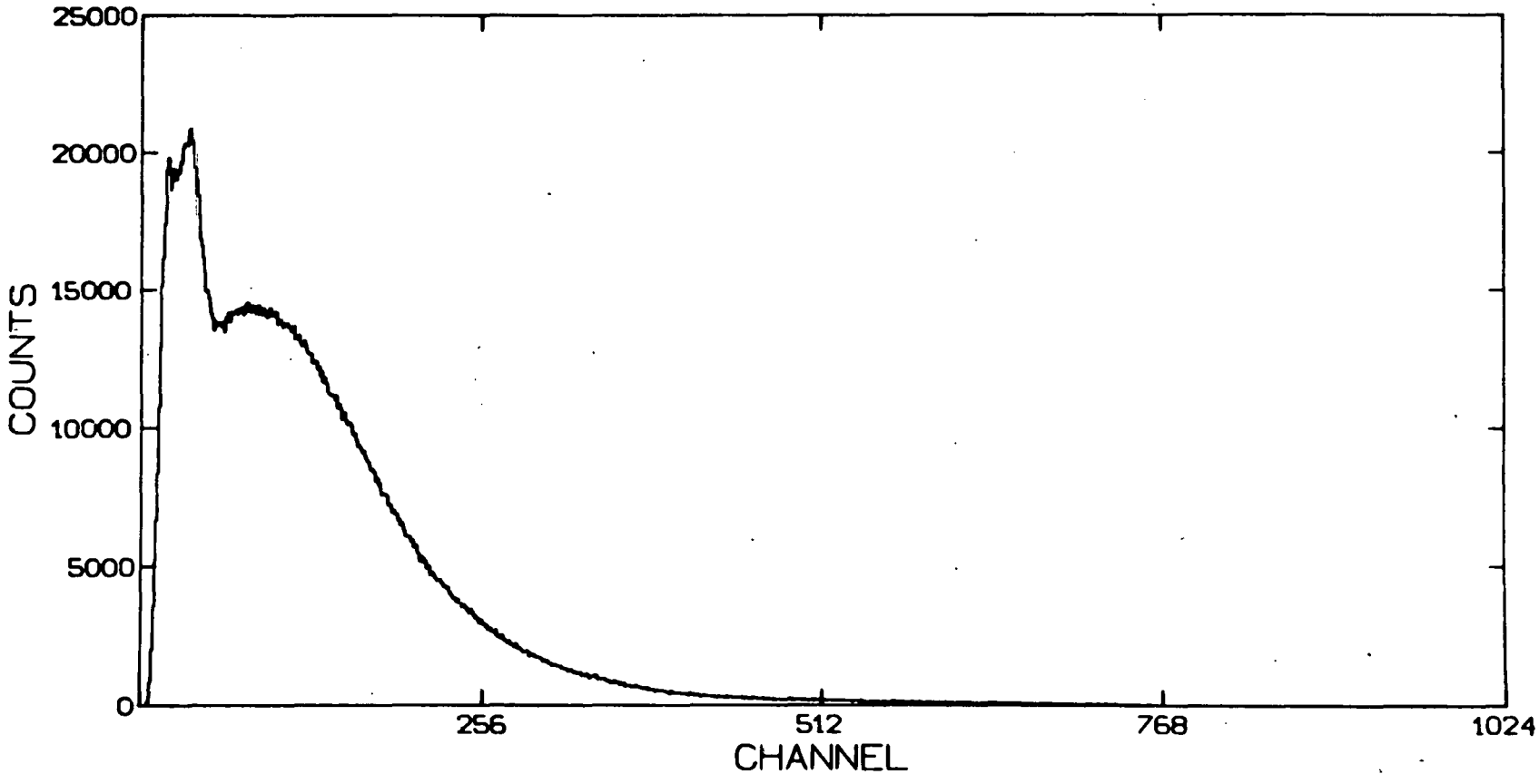
25000
20000
15000
10000
5000
0
COUNTS
256
512
768
1024
CHANNEL

insure that the positrons had been emitted into the solid angle of the telescope and not scattered into the telescope. A routed TAC spectrum consisting of events satisfying both above conditions was then generated.

N_+ and N_- were calculated using the same random background subtraction, normalization and dead-time correction methods that were used for the ^{28}Al analysis. The quantity $\langle v/c \rangle$ was calculated using the allowed shape for the beta spectrum and the stopping power of the surface barrier detector and gave $\langle v/c \rangle = 0.970$. The polarimeter efficiency at 7.068 MeV is 0.03054 ± 0.00072. These values, along with the previous value of $\langle \cos(\theta) \rangle = 0.938$, were used to calculate A.

An additional correction factor for the feeding of the 8.437 MeV state by the Fermi transition to the 9.515 MeV analog state was applied. The feeding of the 8.437 MeV state by the Fermi transition implies $N_{+(-)} = N_{o+(-)} + N_F$ where $N_{o+(-)}$ is the number of detected 7.068 MeV γ rays in the +(-) route from the beta transition directly to the 8.437 MeV state, and N_F is the number of detected 7.068 MeV γ rays from the feeding of the 8.437 MeV state by the Fermi transition. Since the properly normalized and dead-time corrected number of γ rays from the Fermi transition must be isotropic, N_F is the same for both routes. This implies

$$(N_+ - N_-)/(N_+ + N_-) = (N_{o+} - N_{o-})/(N_{o+} + N_{o-} + 2N_F)$$
$$= (N_{o+} - N_{o-})/\{(N_{o+} + N_{o-})(1+F)\}$$

where

$$F = 2N_F/(N_{o+} + N_{o-})$$

$$= \frac{\text{(no. of 7.068 Mev } \gamma\text{'s from the Fermi transition)}}{\text{(no. of 7.068 MeV } \gamma\text{'s from the G-T transition)}}$$

The branching ratio for the Fermi transition is 0.37 (Wa 81), and the branching ratio for the beta transition to the 8.437 MeV state is 0.50 (Wa 81). The γ-ray branching ratio from the 9.515 MeV state to the 8.437 MeV state is 0.41 (Wa 81). These numbers give

$$F = (0.37 \times 0.41)/0.50 = 0.30.$$

Now A is given by

$$A = \frac{N_+ - N_-}{N_+ + N_-} \frac{1}{\eta \langle v/c \rangle \langle \cos(\theta) \rangle} (1 + F) .$$

In the above calculation of the correction factor (1+F) it is assumed that the analog decay is a pure Fermi decay. From the ft value for this decay (see section I.I) we know that M_{GT} for the decay is approximately zero. If the ratio M_{GT}/M_F is 0.2 and the γ-ray transition from the 4^+, 9.515 Mev analog state to the 4^+, 8.437 MeV state is pure M1 the corection factor only changes by 5%. If the γ-ray transition has a small but non-zero E2/M1 mixing ratio, then the change in (1+F) is even smaller.

Using the above equation A was calculated for 88 different runs. The 88 values of A were then weighted by their errors squared and combined to give an overall

$$A = -0.188 \pm 0.039$$

with a χ^2 per degree of freedom of 0.91.

With the appropriate substitutions for the J's and λ, equation I.F-5 relates A to the Fermi matrix element by

$$A = (-0.083 + 0.745y)/(1+y^2)$$

where $y = (G_V M_F)/(G_A M_{GT})$,
and the G's and M's are the coupling constants and reduced matrix elements defined in chapter 1. Solving for y gives

$$y = -0.147 \mp 0.058$$

where $\Delta A = \frac{\partial A}{\partial y} \Delta y$

was used to evaluate the error in y.

Using equation I.F-3 , the measured ft = 8511 seconds (Wa 81), the measured value of y and the sign of M_{GT} from the Nilsson model calculation, one obtains

$$M_F = \sqrt{(2ft(\text{super allowed})/ft)} \times y/\sqrt{(1 + y^2)}$$
$$= -0.124 \pm 0.048$$

where $\Delta M_F = \frac{\partial M_F}{\partial y} \Delta y$

was used to evaluate the error in M_F.

Equation I.F-4 gives for $\langle H_{CD} \rangle$

$$\langle H_{CD} \rangle = -\Delta E \, M_F / \sqrt{2}$$
$$= 1078 \text{ keV } (-0.124) / \sqrt{2}$$
$$= -95 \pm 36 \text{ keV}$$

where ΔE is the perturbation theory energy denominator, and the error in $\langle H_{CD} \rangle$ is given by $\Delta M_F \, \Delta E / \sqrt{2}$.

The β^+ decay to the 4^+, T=0 state at 4.123 MeV was analyzed in a slightly different fashion. The peak in the NaI spectrum for the 2.754 MeV γ ray for the 4.123 MeV $\rightarrow$ 1.369 MeV transition had a considerable background from higher energy γ's. To do a correct background subtraction N_+ and N_- were calculated from routed NaI spectra. The routed NaI spectra were generated by putting a window on the TAC peak in each route and two random background windows on each side of the TAC peak in each route. The total β energy was also constrained to be larger than 6 MeV to eliminate events from other beta branches with lower end-point energies. Four NaI spectra were then produced; one spectrum was for events with high energy betas in the TAC peak in the + route, one spectrum was for events with high energy betas in the TAC background in the + route, one was for events with high energy betas in the TAC peak in the - route, and one was for events with high energy betas in the TAC background in the - route.

The peak area for the 2.754 MeV γ ray was then computed for each of the four spectra by putting a window on the 2.754 MeV peak and an equal size window on the background on the high side of the 2.754 MeV γ peak. The area for each 2.754 MeV γ peak was then computed as (peak window sum) - (background window sum). $N_{+(-)}$ was then computed by taking (peak area for the 2.754 MeV γ in the TAC peak in the +(-) route) - (peak area for the 2.754 MeV γ ray in the TAC background in the +(-) route). N_+ and N_- were then corrected by the same normalization and dead-time correction factors that were used for the beta decay to the 8.437 MeV state. A was calculated for the same 88 runs that were used to calculate A for the decay to the 8.437 MeV state. For the range of beta energies considered $\langle v/c \rangle$ was calculated to be 0.997. For the 2.754 MeV γ ray $\eta = 0.03497 \pm 0.00083$. Using these values one obtains

$$A = -0.201 \pm 0.260$$

which, within the relatively large error bars of the present measurement, agrees with the previous values of -0.089 ± 0.057 (Ha 63) and -0.084 ± 0.054 (Bl 64).

Using the same method of calculation as was used for the decay to the 8.437 MeV state with ft = 1350000 seconds (Wa 81) and $\Delta E = -5392$ keV gives

$$y = -0.165 \pm 0.393$$

$$M_F = -0.0110 \pm 0.0650$$

$$\langle H_{CD} \rangle = -41.9 \pm 248 \text{ keV}.$$

F. Conclusions

The techniques developed in this work for measuring the β-γ circular polarization correlation produced excellent results for decays measured as calibrations. These results demonstrated the high precision of the apparatus developed. With very high confidence in the measurement technique a very large charge-dependent matrix element between the analog state at 9.515 MeV and the suspected anti-analog state at 8.437 MeV was measured.

The result -96 ± 36 keV for the charge-dependent matrix element is consistent with the empirical estimate based on mass splittings (-77 keV) given in chapter I. This is the largest charge-dependent matrix element observed in β decay. The same type of measurement using the β^- decay of ^{24}Na to the 4.123 MeV state in ^{24}Mg, which measures the mixing between the analog and 4.123 MeV state, yielded a charge-dependent matrix element of only 5.4 ± 2.2 keV. The explanation of the large value of -95 ± 36 keV is still unresolved. It seems unlikely that the Coulomb interaction alone can account for this large value and that a short range, $\Delta T=1$ nuclear force is probably responsible for this result.

REFERENCES

Ad 73 E.G. Adelberger, M.D. Cooper and H.E. Swanson, Nuclear Physics Laboratory Annual Report, University of Washington 11, (1973).

Ad 77 E.G. Adelberger, R.E. Marrs, K.A. Snover and J.E. Bussoletti, Phys. Rev C 15, 484, (1977).

Al 79 D.E. Alburger and E.K. Warburton, Phys. Rev. C 20, 793, (1977).

An 69 J.D. Anderson, S.D. Bloom, J. Cerny and W.W. True, Nuclear Isospin, Academic Press, New York, (1969).

Ba 66 F.C. Barker, Nucl. Phys. 83, 418, (1966).

Bl 62 S.D. Bloom, L.G. Mann and J.A. Miskel, Phys. Rev. 125, 2021, (1962).

Bl 64 S.D. Bloom et al., Phys. Rev. 134, B481, (1964).

Bl 81 J.S. Blair, private communication.

Br 66 C.P. Brown, W.D. Callender and J.R. Erskine, Phys. Lett. 23, 371, (1966).

Br 72 W.J. Braithwaite, J.E. Bussoletti, F.E. Cecil and G.T. Garvey, Phys. Rev. Lett. 29, 376, (1972).

Ce 74 F.E. Cecil, L.W. Fagg, W.L. Bendel and E.C. Jones Jr., Phys Rev C 9, 798, (1974).

Ch 65 R.B. Chesler, Nuc. Instr. and Meth. 37, 185, (1965).

De 74 A. DeShalit and H. Feshbach, Theoretical Nuclear Physics, Vol I., John Wiley, New York, (1974).

Di 60 F.S. Dietrich and L. Cranberg, Bull. Am. Phys. Soc. 5, 493, (1960).

Di 78 P.A. Dickey, J.E. Bussoletti and E.G. Adelberger, Nucl. Phys. A303, 442, (1978).

En 78 P.M. Endt and C. Van der Luen, Nuc. Phys. A310, (1978).

Er 61 J.R. Erskine and C.P. Brown, Phys. Rev. 123, 958, (1961).

Er 66 J.R. Erskine and C.P. Brown, Phys. Rev. 143, 683, (1966).

Fo 66 J.D. Fox and D. Robson, Isobaric Spin in Nuclear Physics, Academic Press, New York, (1966).

Ha 63 E.L. Haase, H.A. Hill and D.B. Knudsen, Phys. Lett. 4, 338, (1963).

He 32 W. Heisenberg, Z. Phys 77, 1, (1932). Translated in D.M. Brink, Nuclear Forces, Permagon, Elmsford, N.Y., (1965).

Ho 81 C.D. Hoyle, E.G. Adelberger and A. Ray, to be published.

Ma 65 L.G. Mann, D.C. Camp, J.A. Miskel and R.J. Nagle, Phys. Rev. 137, B1, (1965).

Ma 66 J.B. Marion and M. Wilson, Nucl. Phys. 77, 129, (1966).

Mc 78 A.B. McDonald and E.G. Adelberger, Phys. Rev. Lett. 40, 1692, (1978).

Mo 58 G. Morpurgo, Phys. Rev. 110, 721, (1958).

Pa 68 P. Paul, D. Kohler and K.A. Snover, Phys. Rev. 173, 919, (1968).

Ra 75 S. Raman, T.A. Walkiewicz and H. Behrens, Atomic and Nuclear Data Tables 16, 451, (1975).

Sc 66 H. Schopper, Weak Interactions and Nuclear Beta Decay, North Holland, Amsterdam, (1966).

Sw 69 W.E. Sweeney and J.B. Marion, Phys. Rev. 182, 1007, (1969).

Wa 81 E.K. Wharburton, C.J. Lister, D.E. Alburger and J.W. Olness, Phys. Rev. C 23, 1242, (1981).

Wu 66 C.S. Wu and S.A. Moszkowski, Beta Decay, Interscience, John Wiley, New York, (1966).

VITA

Charles David Hoyle was born to Charles and Bonnie Hoyle on [redacted] He graduated from The Columbus Academy then attended Princeton University where he received his A.B. degree in Physics in 1973. From 1973 to 1977 he taught physics at the U.S. Naval Nuclear Power school. After leaving the Navy he attended the University of Washington and joined the Nuclear Physics Laboratory.